Characterisation of a Retro-Fit Engine Intake Water Doping Device for Improved Urban Air Quality

A thesis submitted for the degree of Masters of Science in

Engineering with Innovation and Entrepreneurship

by

Seifeldin Mohamed Said Mattar, BEng (Hons)

Department of Mechanical Engineering University College London

I, Seifeldin Mohamed Said Mattar, confirm that the work presented in this thesis is my own. Where information has been derived from other sources, I confirm that this has been indicated in the thesis.

September 2018

Word Count: 11989

Abstract

A novel intake manifold water injection device that has emerged for its special abilities in emission reductions is the Econokit. The Econokits performance in reducing emissions has varied however and the gas outputs that it injects into the intake manifold are yet to be known. Therefore, this project characterises the Econokit device to understand its gas outputs and to understand why its performance varies from one engine to the other.

An experimental bench was set up to simulate the same conditions that the Econokit experiences in a car engine. These conditions were varied and using a humidity sensor and gas analyser the gas composition of the Econokits output was analysed. From the results it was seen that as the bubbler temperature was increased, the water content in the Econokit output air flow also increased. It was also seen that the Econokits reactor does indeed change the air flow composition. When high temperatures were applied to the reactor, from 200-450 °C, both CO, up to 192 ppm, and CO_2, up to 5100 ppm, were detected. From reactor temperatures of 410 C°, there was also a slight detection of H2, up to only 13 ppm.

The changes in gas composition noticed for the outputs at the high reactor temperatures give an indication as to why the Econokit is more effective on some engines than others, it has shown that the temperatures that the Econokit is being subjected to has a huge effect on; tthe water content it injects, the gas outputs it injects and on its performance in reducing engine emissions.

Acknowledgments

I would like to thank and acknowledge my supervisor, Dr Paul Hellier, for his unparalleled guidance and support throughout the entirety of this project. I am also grateful for Dr Hellier and UCL for providing such a challenging and exiting project and for allowing me to use the experimental equipment required for the completion of the project.

Table of Contents

Nomenclature

CI	Compression Ignition
CO	Carbon Monoxide
CO$_2$	Carbon Dioxide
CV	Co-efficient of Variance
DI	Direct Injection
Dr	Dilution Ratio
DWI	Direct Water Injection
EGR	Exhaust Gas Recirculation
H$_2$O	Water
HFO	Heavy Fuel Oil
HC	Hydrocarbon
IMWI	Intake Manifold Water Injection
IMI	Intake Manifold Injection
LFO	Light Fuel Oil
N$_2$	Nitrogen
NO	Nitric Oxide
NOx	Nitrogen Oxides
PM	Particulate Matter
SD	Standard Deviation
SI	Spark Ignition
SO$_2$	Sulphur Dioxide
WI	Water Injection

List of Tables

List of Figures

1 Introduction

Greenhouse gas emissions and harmful air pollutants represent an ongoing, evolving threat on worldwide human health and well-being. Emission levels have increased by 80% since 1970 [International Energy Agency 12], causing; a constant increase in global warming, smog and ozone air pollution and most importantly an overall deterioration in average human health and average human life expectancy [Government of Canada 2017; What's Your Impact 18]. Transportation presents a major source of greenhouse gas emissions, it is the largest contributor to harmful emissions in the UK at 26% of total greenhouse gas emissions [Gabbattis 18], as well as the largest contributor in the US at 28% of total emissions [EPA 18]. On the global scale, emissions from transportation accounts to 14% of all greenhouse gas emissions [EPA 18].

Emissions from transportation, produced from petrol and diesel engines are particularly dangerous on human health. Harmful emissions from transportation include; carbon monoxide, nitrogen oxides, particulate matter and hydrocarbons [Vehicle Certificate Agency 18]. These gases, if inhaled, will block the passage of oxygen from the heart and the brain, they would also result in lung irritation and respiratory illness [Vehicle Certificate Agency 18; Union of Concerned Scientists 18]. Particulate matter in particular can also penetrate deep into the lungs and cause deaths in many occasions. In the UK alone for example, 29000 deaths a year are credited to particulate matter pollution [Public Health England 14].

Measures are therefore being taken to try and limit the level of emissions. The introduction of electric vehicles has been a major factor in attempts to reduce emission levels. Electric vehicles can emit less than half the amount of emissions that are emitted from petrol and diesel engines [Neslen 18]. However, electric vehicles only account to a very small percentage of total vehicles in use, for example, in the UK, in 2018, only about 0.53% of total vehicles in use will be electric [Department for Transport 18; Hull 18]. The percentage of electrical vehicles in use is even lower in the less developed countries [Statista 2018], and only by 2040 is electric vehicles expected to be the primary source of transportation [Leahy 18].

Consequently, in an attempt to lower emission levels, governments have been introducing emission standards to limit the maximum amount of emissions from vehicles [Government of Canada, 2018]. To meet the new government emission standards, new techniques and innovations are constantly being studied and developed. A technique that has been proven to reduce harmful gas emissions in vehicles is water injection. Water injection has proven to cause a decrease in levels of emissions from exhausts when applied to engines [Tauzia, Maiboom and Shah 10].

A newly developed water injection retro-fit device is the Econokit. Econokit has shown very promising results in reducing harmful gas emissions. Econokit manufacturer, Econokit France [2018], claim that through testing the Econokits performance on a 1.4l turbo diesel engine with Bureau Veritas [2018], the Econokit was able to reduce; CO_2 emissions by 15.5%, NOx emissions by 33.9%, CO emissions by 17.3% and carbon particles by 73.4%. However, the results for Econokit have varied, where it has provided very positive results in terms of emission reduction upon testing on some vehicles, and then results that are not to the same standard when tested on other vehicles [Lindley 16]. The reasons for the variation in Econokit emission reduction performance has yet to be fully determined.

Therefore, this study aims to characterise the Econokit device to further understand it and to understand at what conditions it functions to its maximum capabilities. Econokit is a retro-fit water doping system for combustion engines that improves combustion efficiency by increasing the humidity rate and modifying the gas composition of air that is injected into the air intake manifold [Econokit France 18]. Figure 1 below shows the main components of the Econokit device.

Figure 1. Econokit Components [Econokit India 13]

As seen in Figure 1 above, Econokit consists of a water tank, which acts as the bubbler. This is fitted in the vehicle's bonnet and placed in a hot area to allow the water in the tank to heat up. It also consists of, from right to left; a hose which is used for the air flow, clamps to hold the hose and tighten it onto the other components, the reactor which allows the processing of the humid air, the diffuser which inserts the humid processed air flow into the air intake manifold and additional fixtures to aid assembly.
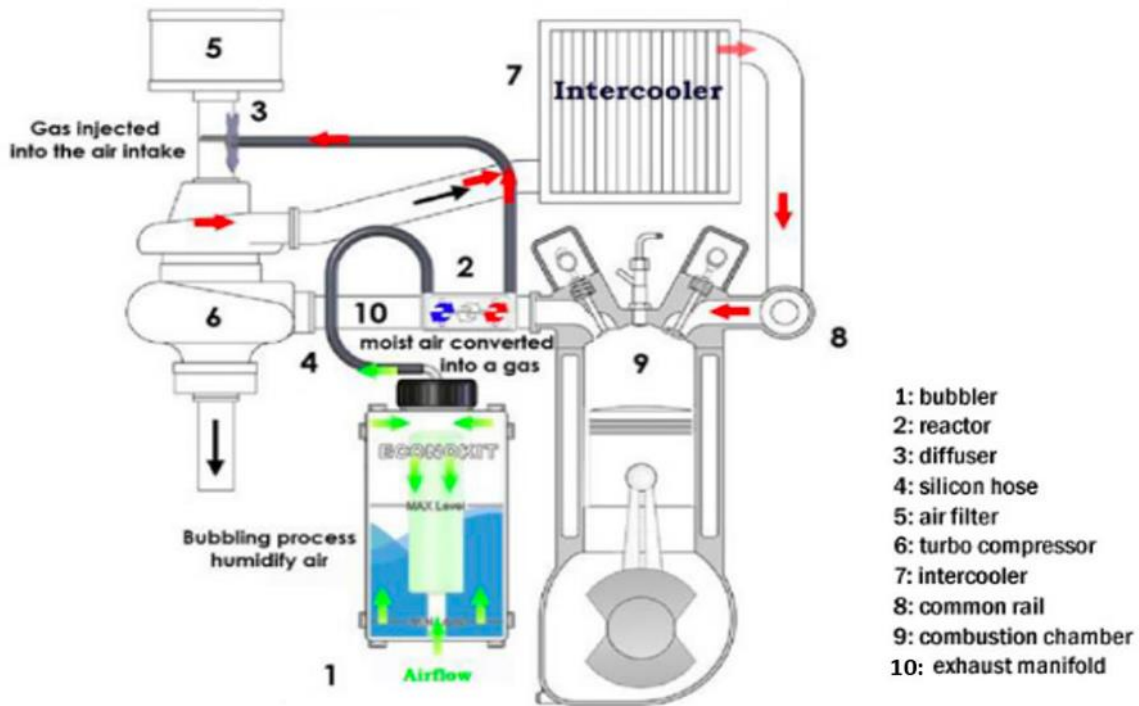
Figure 2. Econokit Air Flow [Econokit India 13]

Figure 2 above shows how the Econokit operates. As seen in figure 2, through a hole situated at the bottom of the bubbler, air is pulled into it. The air then bubbles through the hot water inside of it. The humid air then exits the bubbler and flows within the hose and through the reactor which is clamped onto the exhaust manifold. The reactor then gains heat from the exhaust manifold which is used to processes the vaporised water. The placement of the reactor onto the exhaust manifold also allows for the polarisation of the water molecules within the humid air flow going through it [Econokit France 18]. The humid air and the produced gas then exit the reactor and flow through the diffuser into the air intake manifold. The introduction of the water molecules and the processed gas into the air intake manifold helps in controlling the temperature and pressure of combustion to reduce the harmful exhaust gas emissions [Econokit France 18].

2 Aims and Objectives

The aim of this thesis is to characterise and understand the Econokit device by; setting up a test bench to simulate the same conditions that the Econokit experiences in a car engine, then analysing the Econokits outputs as these engine conditions are varied.

The objectives include:

- Conducting extensive literature review on; emissions improvement systems, water injection systems, the effect of intake manifold water injection on engine emissions and on the Econokits catalytic reactor, to improve current knowledge on the Econokit system and to identify further gaps in literature that could be explored.
- Designing a test bench experiment to simulate the conditions that the Econokit would experience in a car engine while retaining the ability to vary these conditions.
- By varying the bubbler temperature, analyse its effect on Econokit injected water content and water injection rate.
- Analyse the Econokit output air flow composition as the reactor temperature is varied.
- Observe and explain the results that emerge from the tests.
- Use the literature review and the test results to identify; what differs the Econokit from other intake manifold water injection systems, and why the Econokits performance in reducing emissions has varied.

3 Literature Review

The literature being reviewed here focuses on gathering and analysing information that is relevant to understanding and testing the Econokit system.

3.1 Emission Improvement Systems

Econokit is, as mentioned earlier, an innovative water injection device that is used to reduce exhaust emissions. There are however other systems and methods currently used to reduce engine emissions. This includes exhaust gas recirculation (EGR) and post-composition control methods. These methods are discussed and explained in this section to be able to compare them with water injection and the Econokit device later in the study.

3.1.1 Exhaust Gas Recirculation (EGR)

Exhaust gas recirculation (EGR) is a system used to reduce NOx emissions from engines [Zheng, Reader and Hawley 04]. The system is implemented by taking a portion, about 10-25%, of the exhaust gas and re-rerouting it into the inlet manifold [Fernando, Hall and Jha 06]. The exhaust gas being re-circulated into the inlet is inert and so it does not react in the combustion chamber [Fernando, Hall and Jha 06]. The inert exhaust gas replaces a portion of the intake air and causes a reduction in the concentration of oxygen [Khalilarya et al 11]. A lower oxygen concentration means that the combustion becomes slower and the heat release rate slows down and so the in-cylinder temperature decreases [Sher 98; Khalilarya et al 11]. Also, the specific heat capacity of the inert exhaust gas is higher than the specific heat capacity of the oxygen and nitrogen in the intake air, and so the injection of exhaust gas increases the overall heat capacity of the inlet cylinder charge, which also results in a lower in-cylinder temperature [Zheng, Reader and Hawley 04]. Since NOx formation requires high energy, which is obtained from high temperatures, a lower in-cylinder temperature would mean that there would be less NOx formation [Tesfa et al 12].

By using EGR, up to 50% reductions in NOx emissions can be achieved [Tesfa et al 12]. Using EGR would also reduce knocking tendency and it would allow the engine to operate under a higher compression ratio [Ibrahim and Bari 09]. It does however have some major drawbacks, for example when high-pressure EGR is used, some components in the engine

might get damaged when exposed to the un-processed exhaust gases [Mira LTD and PBA 02]. The other main drawback of EGR is that even though it reduces NOx emissions, it increases other emissions, especially PM emissions [Tauzia, Maiboom and Shah 10].

3.1.2 Post-composition Control Methods

The other main method used to reduce emissions is post combustion control of the exhaust gases. A way of controlling the exhaust gases is using a catalytic converter. A three-point catalytic converter for example can be used to convert emissions of; NOx to N_2, unburned hydrocarbons into H_2O and CO to CO_2 [Fernando, Hall and Jha 06]. There are however drawbacks to using catalytic converters, these include that the materials used in catalytic converters are palladium, platinum, and rhodium, which are all very expensive [Tesfa et al 12]. Another drawback is that the catalytic converters work best with a stoichiometric air to fuel ratio of about 14.7:1 [Fernando, Hall and Jha 06]. Diesel engines however tend to run lean, running lean makes the catalytic converters less efficient and less effective in reducing NOx emissions. Running lean also means that the engine temperature is higher and a higher engine temperature results in more NOx formation [Fernando, Hall and Jha 06].

3.2 Water Injection

Water injection, which is also known as Anti-Detonant Injection (ADI), was found in the 1920s, it is a method that involves adding water to the cylinder and fuel-air mixture of engines to cool the combustion chamber [Babu, Amba Prasad Rao and Hari Prasad, 2015]. There are two main methods of WI; direct water injection and intake manifold water injection. Both direct and indirect injection are discussed in detail in the following sections.

3.2.1 Direct Water Injection

Direct water injection (DWI) is a form of WI where the water is directly injected into the combustion chamber [Wartsila 18]. It is a method used to increase fuel efficiency and decrease emission outputs. Both water and fuel are injected using a combined injection valve, one needle injects the water and the other injects the fuel [Wartsila 18]. Water is injected into the combustion chamber first to cool it down, then the injection of fuel follows [Wartsila 18]. The water to fuel ratio is adjusted and controlled by modifying the duration of injection [Wartsila 18]. The ability to adjust the water to fuel ratio acts as an advantage for direct water

injection as the ratio can be modified in accordance to the engine loads and in accordance to the required engine outputs in terms of performance and emissions [Zhang et al 2017].

The main function of DWI is to reduce exhaust gas emissions. This is achieved through the injected water absorbing heat and decreasing the local adiabatic flame temperature in the combustion chamber [Tesfa et al 12]. The formation reaction of NOx requires a high activation energy, energy for NOx formation is obtained from the peak flame temperature, and so when the peak flame temperature is reduced through the injected water, NOx emissions are also reduced [Tesfa et al 12]. Through the lower combustion temperatures, better fuel economy for the engine can also be achieved [Collie 18].

The exact effects of direct water injection on engine performance and emission outputs have been studied and analysed upon being installed on different engines. Tschalamoff et al [2007] examined the effects of DWI on a turbocharged 13.6 litre natural gas engine. By using a water to fuel ratio of 1 to 5, Tschalamoff et al [2007] observed a reduction of 50% in NOx emissions. However, although a significant reduction in NOx was observed, a small increase in HC and CO emissions was also observed as well as a lower engine efficiency [Tschalamoff, Laaß and Janicke 07]. The lower engine efficiency is a result of slower combustion and lower combustion temperature which is induced by the addition of water into the intake manifold [Tschalamoff, Laaß and Janicke 07].

Sarvi et al [2009] also investigated the effects of DWI, this time on a turbo charged diesel engine, emission tests were performed on the engine with different loads and by using different types of fuel, light fuel oil (LFO) and heavy fuel oil (HFO) (characteristics for both types of fuel is shown in appendix 1). In agreement with Tschalamoff et al [2007] results, Arto Sarvi et al [2009] also noticed a significant decrease in NOx emissions. As seen from the results shown in figure 3 below, the NOx emissions were reduced by an average of 35% on the different tests with the different fuel types and engine loads, where the reduction reached up to 50-60% in some occasions. What they did notice however, is that for the engine operating on a low load while using HFO, the effect of DWI on NOx emissions was minimal. Therefore, from Sarvi et al [2009] results, shown in figure 3, it can be seen that engine load has a huge effect on DWI performance, DWI becomes effective in reducing NOx emissions at high loads where it can be ineffective at lower loads. Sarvi et al [2009] results, figure 3 below, also show that the type of fuel being used on the engine also has an

15

implication on the effectiveness of DWI in NOx reduction, when LFO was used a lower NOx emission is observed than when HFO is used. This is due the lower cetane number of LFO than HFO [Sarvi, Kilpinen and Zevenhoven 09].
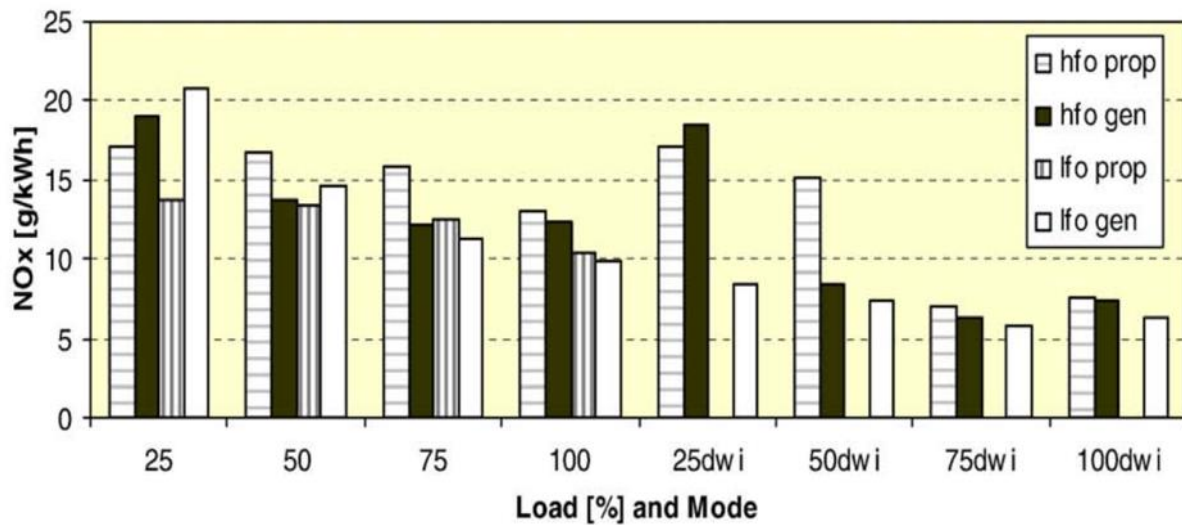
Figure 3. NOx emissions with/without DWI on a diesel engine vs. engine load and operation mode (propulsion and generator) and fuel type (LFO and HFO) [Sarvi, Kilpinen and Zevenhoven 09].

As for other harmful emissions, Sarvi et al [2009] observed an increase of; 10% in CO emissions, 15% in soot and 10% in PM. Therefore, it can be seen that although DWI can reduce NOx emissions significantly, it will increase CO, soot and PM emissions.

3.2.2 Intake Manifold Water Injection

The Econokit, studied in this project, is a novel form of an indirect water injection system (IMWI), and therefore, IMWI is carefully reviewed and studied in this paper. This section focuses on the method by which IMWI affects emissions and section 3.3 focuses on the actual effect of IMWI on each of the emissions.

IMWI is a form of water injection where the water is injected directly into the intake manifold. When IMWI is introduced onto an engine, it has three main effects on it, it is these effects that allow IMWI to cause a reduction in engine emissions. The first effect is the thermal effect. As discussed for DWI in the previous section, the thermal effect involves IMWI lowering the flame temperature, lower flame temperature then results in less NOx formation [Ma et al 14]. The second effect that IMWI has on an engine is the chemical effect, the chemical effect only has a small impact on engine emissions and combustion. It is the effect associated with the increase in OH radicals as a result of water injection, OH radicals

16

contribute in soot oxidation which results in a reduction of overall soot emissions [Farag et al 17]. The final effect that IMWI has on an engine is the dilution effect. This involves the cooling of the intake charge and occurs due to the endothermal process caused by the evaporating water upon in the intake manifold [Arruga et al 17]. The cooling of the intake charge results in the density of the in-cylinder air to increase [Farag et al 17]. The total injected mass then increases at the same volume, water then vaporises in the droplets of fuel as the fuel droplets are being heated, causing a sudden expansion [Greeves, Khan and Onion, 77; Farag et al 17]. The expansion then causes a drop in the in-cylinder pressure. The dilution effect therefore results in a huge decrease in both the in-cylinder pressure and temperature [Farag et al 17]. The dilution effect also improves the mixing of air and fuel before combustion [Farag et al 17]. The reduction in pressure and temperature, as well as the enhanced air and fuel mixing allow the dilution effect to have a huge influence in reducing both NOx emissions and soot formation [Farag et al 17].

The reason as to why water is injected into the intake manifold and not another element is because, out of the elements, water causes the most significant decrease in in-cylinder temperature and pressure when injected [Ma et al 14]. This is mainly attributed to the high specific heat capacity and high latent heat of vaporisation of water in comparison with the other elements [Farag et al 17]. To analyse the effects of using water in comparison to using other elements for intake manifold injection (IMI) and to also demonstrate the thermal, chemical and dilution effects induced by IMWI, Ma et al [2014] used different compositions of water, oxygen and nitrogen for IMI and measured the in-cylinder pressure, temperature and NOx emissions. From Ma et al [2014] results, shown in figures 4 and 5 below, it can be seen that the in-cylinder pressure and temperature were both lowered when a percentage of oxygen was replaced with either water or nitrogen in the intake charge. The significant difference in reduction in in-cylinder pressure and temperature is due to the water and nitrogen having the ability to induce the dilution effect once introduced into the manifold, whereas oxygen on the other hand, when introduced into the manifold, it does not induce the dilution effect [Ma et al 14].
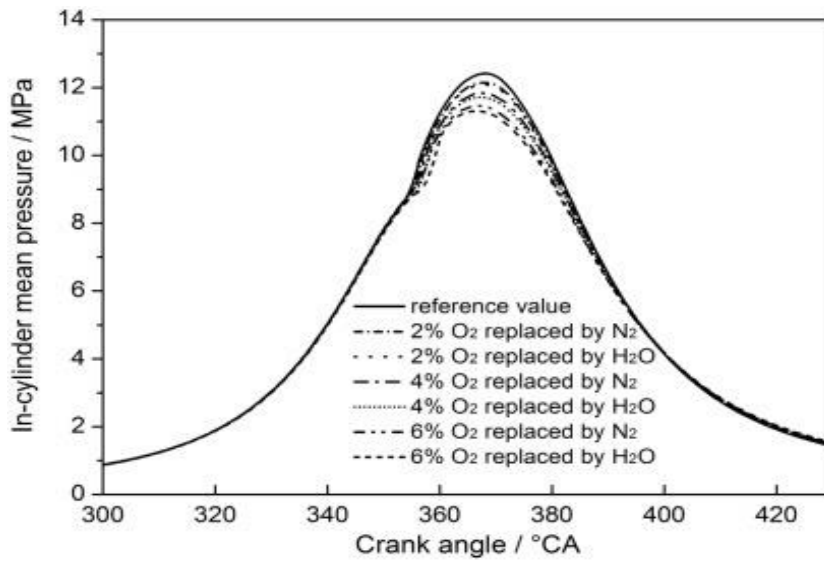
Figure 4. In-cylinder pressure vs crank angle for different intake manifold injection compositions [Ma et al 14].
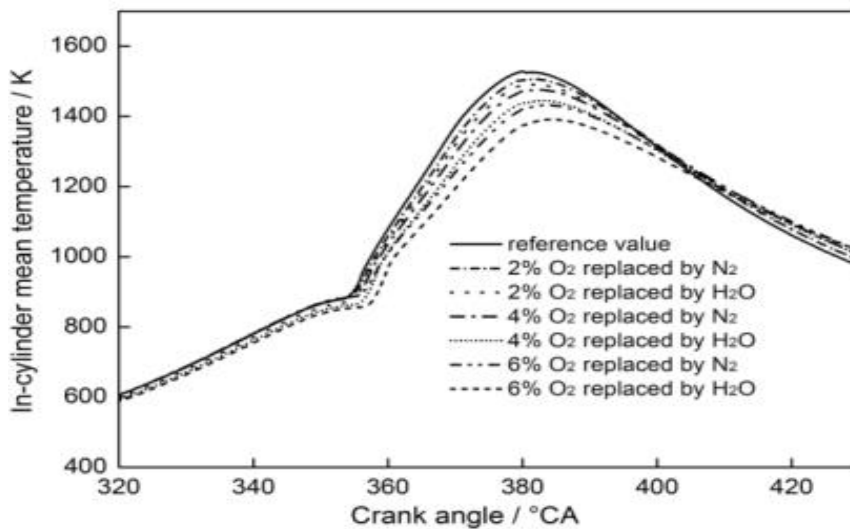
Figure 5. In-cylinder temperature vs crank angle for different intake manifold injection compositions [Ma et al 14].

From Ma et al [2007] results of engine NOx emissions at different inlet charge compositions, shown in figure 6 below, it can be seen that although both water and nitrogen injection induce the dilution effect, as discussed above, the injection of water has the largest effect on reducing NOx emissions. This is due to the chemical and thermal effects of water injection that have been discussed earlier. Since the dilution effect has the largest influence on NOx emissions as concluded by Tauzia et al [2009] and Farag et al [2017], only a small, but important difference in reduction in emissions is caused by using water instead of nitrogen in the inlet charge, as seen in figure 6 below.
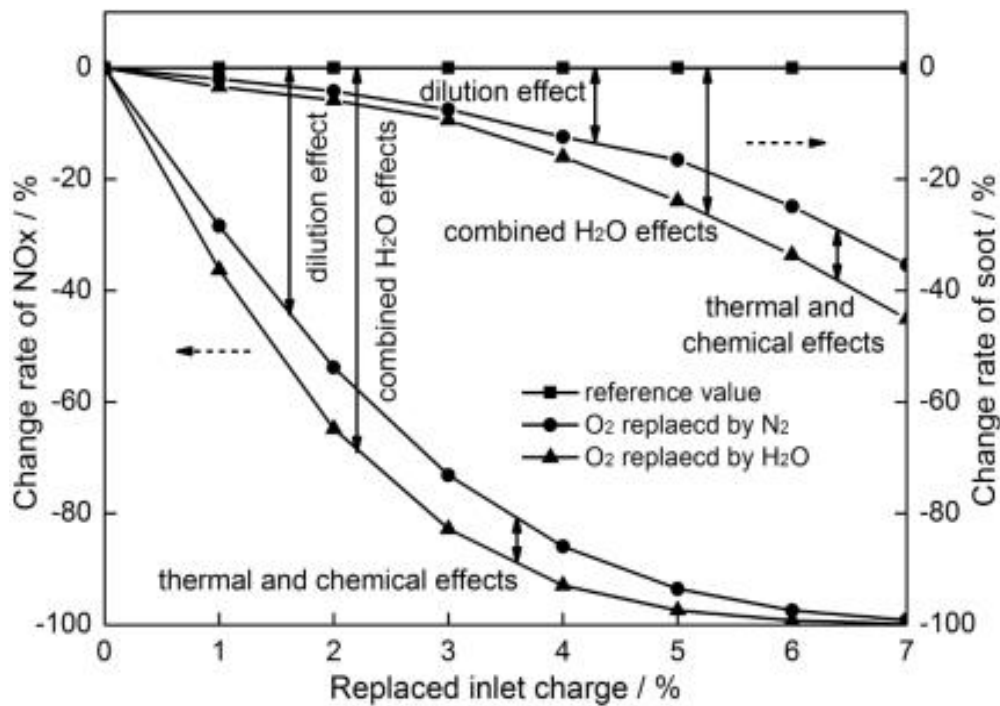
Figure 6. Change rate of NOx and soot emissions vs inlet charge composition
[Ma et al 14].

3.3 Effect of IMWI on Emission Reduction

This section carefully studies and analyses the effect of using IMWI on each of the different exhaust emissions.

3.3.1 Effect of IMWI on NOx Emissions

Through reducing the in-cylinder pressure and temperature as well as through the thermal, chemical and dilution effects discussed in section 3.2.2 above, IMWI can drastically reduce the engines NOx emissions [Ma et al 14]. Upon testing IMWI on a hydrogen-fuelled engine, Subramanian et al [2007] were able to realise a 32% reduction in NO emissions without any losses in break thermal efficiency. Tauzia et al [2009] also experienced up to 50% reductions in NOx emission when they applied the IMWI system on a direct injection diesel engine.

The effect of IMWI on NOx emissions however depends significantly on the rate of water injection. To analyse the effect of the rate of water injection on engine NOx emissions, Tauzia et al [2009] applied an IMWI system onto a direct injection diesel engine, NOx emissions were recorded at different water injection rates for the diesel engine operating under four different loads, **a-d**, as shown in figure 7 below. To compare with the IMWI system, the emissions produced for the same engine but with the EGR system applied is also

shown on figure 7 below. As seen in figure 7, the results obtained by Tauzia et al [2009] agree with Subramanian et al [2007] in that using IMWI results in a significant reduction in NOx emissions. The reduction was observed for all 4 engine loads, with load **a** being the lowest engine load and load **d** being the highest (operating loads used by Tauzia et al [2009] are given in appendix 2). What is more important is that from Tauzia et al [2009] results, figure 7, it can be seen that as the rate of water injection increases, the NOx emissions decrease. It is also seen that IMWI, when compared with EGR, performs better in reducing NOx emissions.
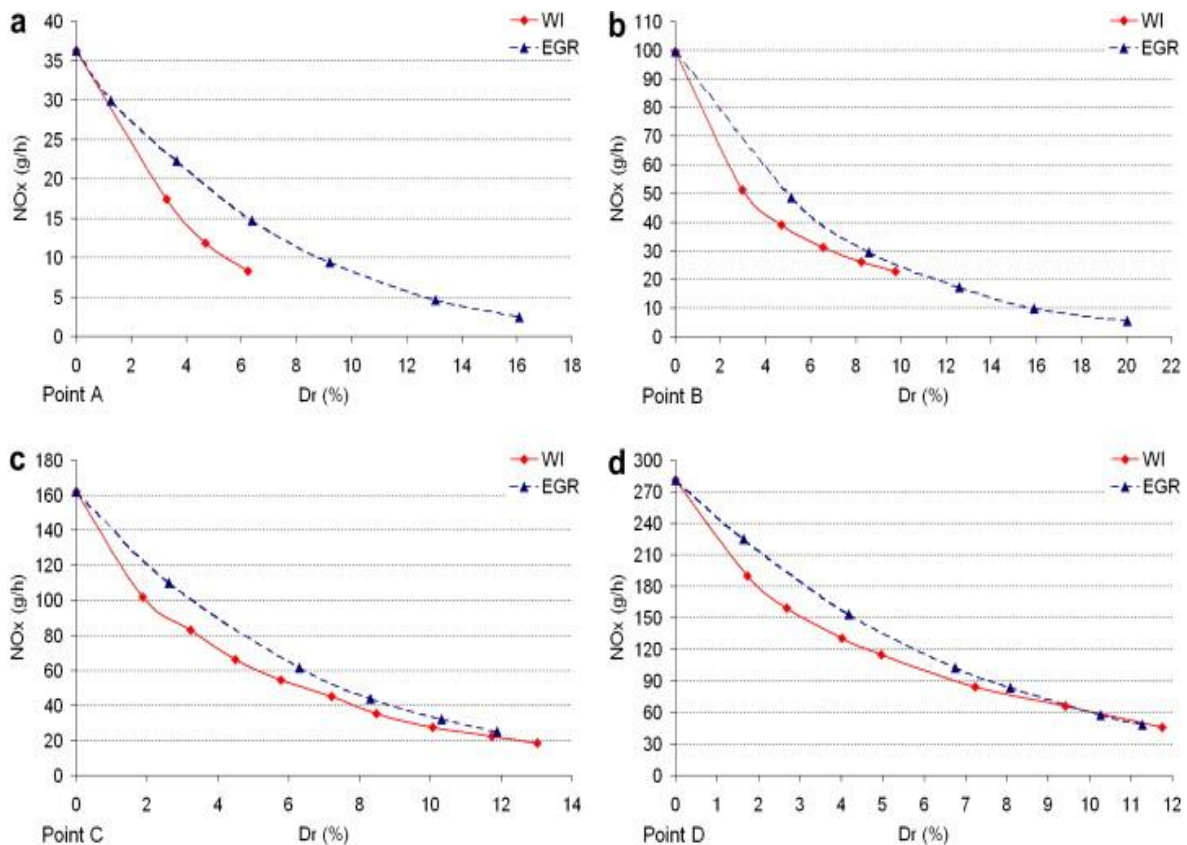
Figure 7. NOx emissions vs WI rate (Dr %) for operating loads **a-d** - comparison with EGR [Tauzia, Maiboom and Shah 10].

As seen from the results observed by Tauzia et al [2009], figure 7 above, the effect of IMWI on NOx emission reduction also depends on the engine's operating engine load. As the engine load or engine speed increases, the NOx emissions also increase. This is due to the NOx emissions depending on engine temperature, and so when the load increases, the engine temperature increases which results in higher NOx emissions [Babu, Amba Prasad Rao and Hari Prasad, 2015]. Babu et al [2015] tested the IMWI on a spark ignition engine and measured the NOx emission levels as the engine speed was varied. From the results obtained

by Babu et al [2015], shown in figure 8 below, it can be seen that IMWI decreases NOx emissions at all engine speeds. More interestingly, it is seen that IMWI has the highest effect on NOx emissions when the engine is operating at medium speeds. The highest reductions in NOx emissions were observed by Babu et al [2015] when the engine was operating at speeds between 3000 rpm and 4500 rpm.
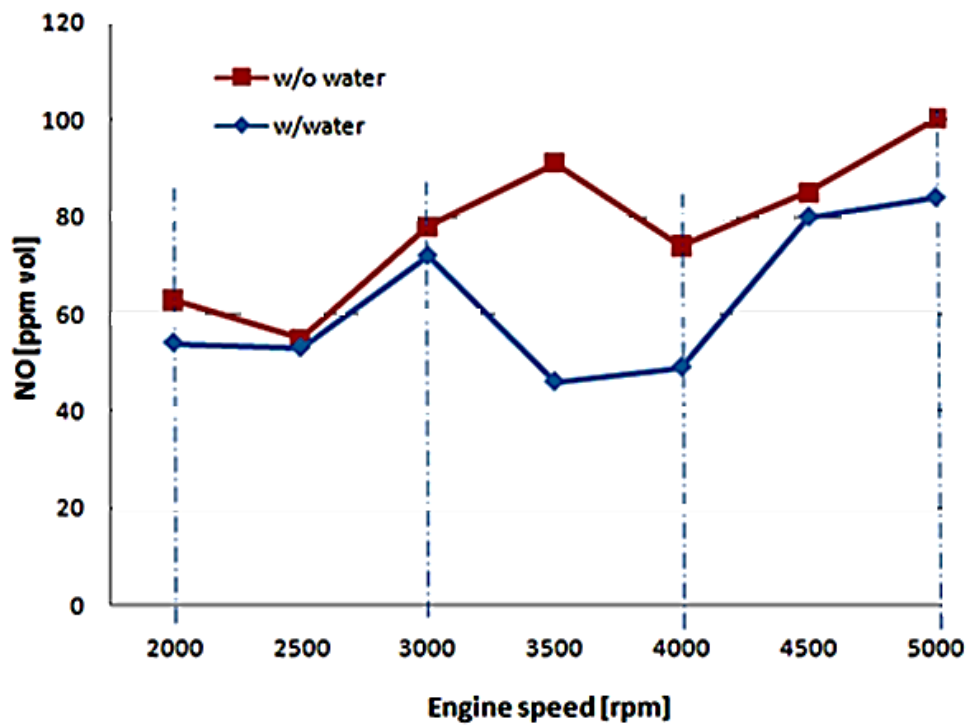
Figure 8. NO emissions vs engine speed with and without IMWI [Babu, Amba Prasad Rao and Hari Prasad, 2015]

Another factor that influences the performance of an IMWI system on NOx emission reduction is the combustion phasing [Arruga et al 17]. Arruga et al [2017] applied IMWI on a spark ignition, NOx emissions were then observed as the combustion phasing was varied. Combustion phasing, which is the time in the engine cycle while combustion occurs [Wildhaber 11], was varied by Arruga et al [2017] through changing the air/fuel ratio and the spark timing. From the results observed by Arruga et al [2017], shown in figure 9 below, it can be seen that IMWI will reduce NOx emissions of ignition engines operating under any combustion phasing, also seen is that the lower the combustion phasing is, the higher the NOx emissions will be.
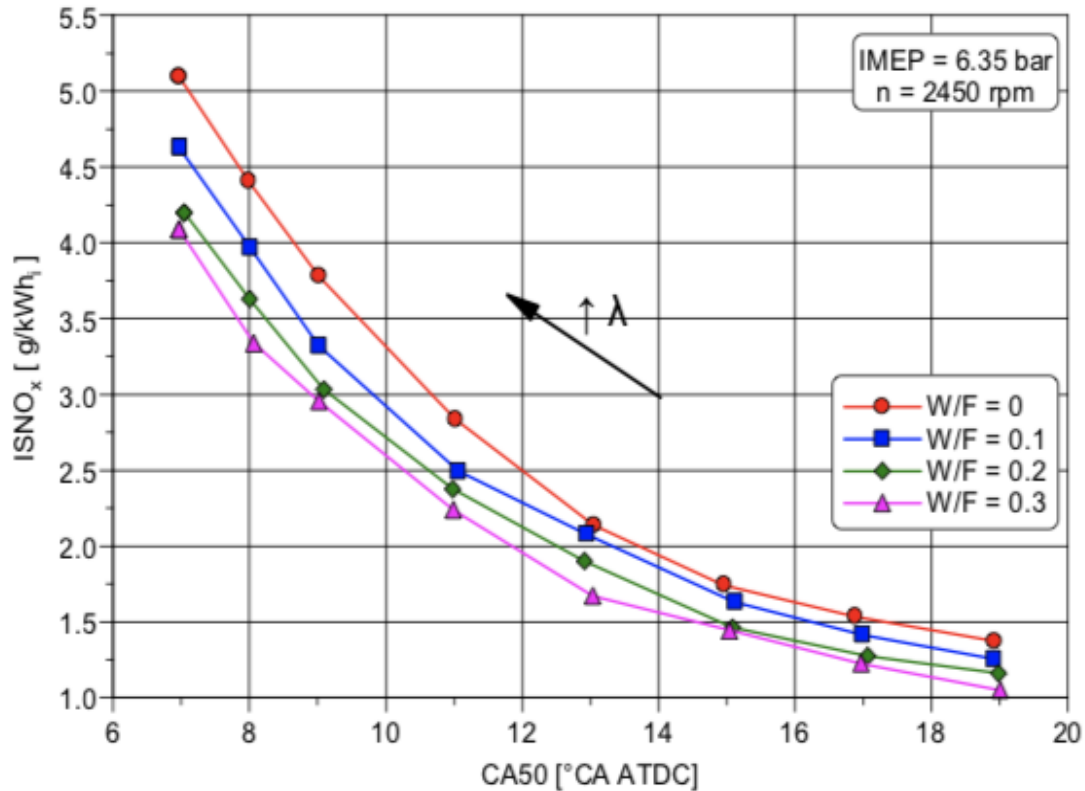
Figure 9. NOx emissions vs combustion phasing CA50 [Arruga et al 2017].

3.3.2 Effect of IMWI on CO Emissions

Intake manifold water injection also has an effect on the CO emissions of an engine. As with NOx emissions, the effect of IMWI on the CO emissions also depends on the engine load, engine speed and rate of water injection.

IMWI was applied onto a compression ignition engine by Tesfa et al [2012] to analyse the effect it has on the engine's CO emissions. CO emission levels were measured by Tesfa et al [2012] for the CI engine operating under two different loads while the engine speed was varied as two different water injection rates were used. From the results obtained by Tesfa et al [2012], presented in figures 10 a-d below, it can be concluded that IMWI has a negative effect on CO emissions. When IMWI was added to the CI engine, the CO emissions increased. The increase in CO emissions were also seen to increase as the water injection rate increased, as seen in figures 10 a-d. This is because, as explained earlier, the injection of water results in a reduction in pre-combustion temperature, although the reduction in pre-combustion temperature reduces the NOx formation as seen in section 3.3.1 above, it does the contrary with CO emissions [Tesfa et al 12]. As the combustion temperatures decrease,

the chemical conversion of CO to CO_2 slows down and so less CO is converted to the less harmful CO_2 [Tesfa et al 12]. It is also seen that at higher engine loads and higher engine speeds, the CO emissions are lower, this is because at the higher speeds and engine loads, the engine temperature is higher, and again, with the higher temperatures more CO converts to CO_2 [Tesfa et al 12].
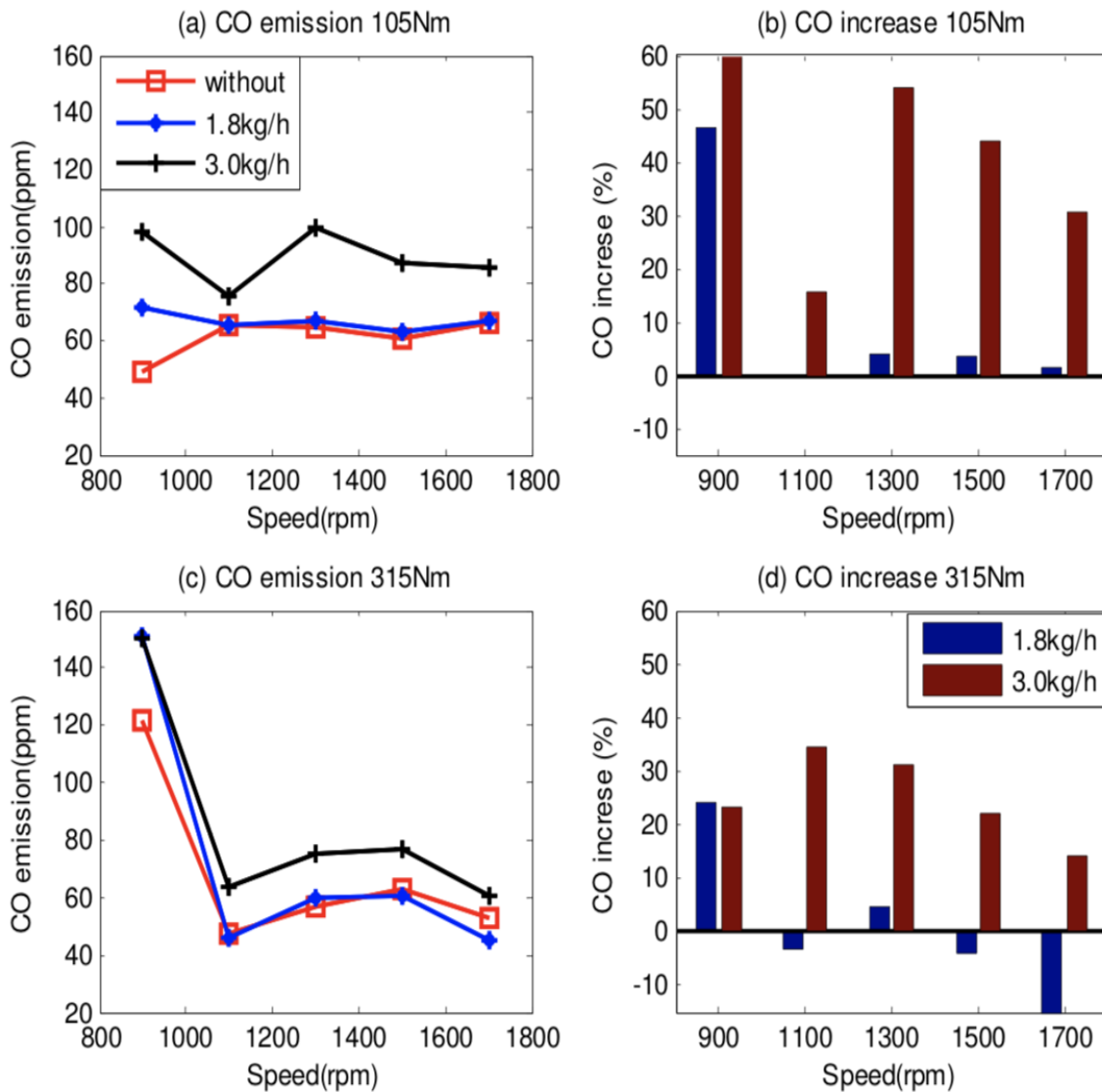
Figure 10. CO emission vs engine speed and CO percentage increase for two different engine loads and two water injection rated [Tesfa et al 2012].

Babu et al [2015] however disagree with Tesfa et al [2012]. Upon applying IMWI onto a spark ignition engine, Babu et al [2015] only experienced a very slight increase in CO emissions at high engine speeds, at all other engine speeds CO emissions did not increase, as seen in figure 11 below.
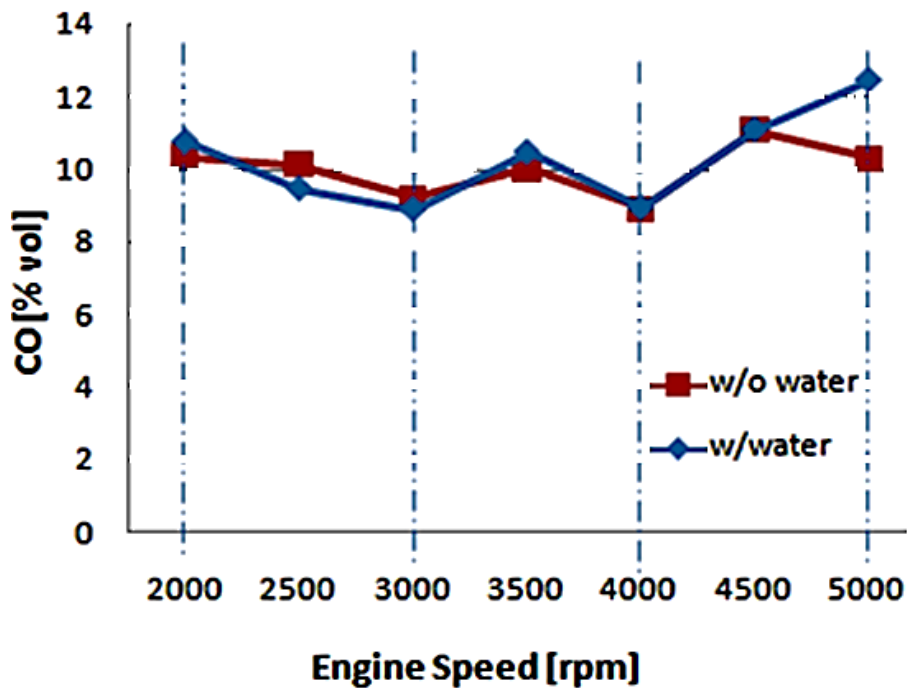
Figure 11. CO emission vs engine speed with and without IMWI for a SI engine [Babu et al 2015]

Overall, as seen, in most occasions IMWI results in an increase in CO emissions, however not always, as IMWI's effect on CO emissions depends on, as discussed above, WI rate, engine type, engine speed and engine Load.

3.3.3 Effect of IMWI on PM Emissions

IMWI also has a huge influence on particulate matter emission. In most occasions, applying water injection results in an increase in PM emissions [Farag et al 17; Kettner et al 16; Tauzia, Maiboom and Shah 10]. This is because, as explained earlier, water injection results in a reduction in temperature. A reduction in temperature limits soot oxidation which in turn results in more PM exiting into the atmosphere from the engine exhaust [Tauzia, Maiboom and Shah 10].

To understand the effect of IMWI on PM emissions, Tauzia et al [2009] applied an IMWI system onto a DI diesel engine. PM emissions were observed for four different engine loads **a-d**, **a** being the lowest load and **d** the highest, as the water injection rate was varied. Results were also compared with the effect of EGR on PM emissions when added onto the same engine. From the results observed by Tauzia et al [2009], shown in figure 12 below, it can be seen that IMWI increased the PM emissions for the higher loads **b**, **c** and **d** (engine loads are shown in appendix 2). As seen in figure 12 below, as the operating load of an engine is

higher, IMWI causes a larger percentage increase in PM emissions. This is because at higher loads the engine temperature is higher, WI causes a larger temperature reduction when the engine temperature is already at a high level, this results in, as explained, less soot oxidising and so more PM exiting from the exhaust [Tauzia, Maiboom and Shah 10]. Another reason as to why IMWI causes an increase in PM emissions is that IMWI also affects the air to fuel ratio [Tauzia, Maiboom and Shah 10]. A slight decrease in the air to fuel ratio, of about 5-7% was observed by Tauzia et al [2009] when the IMWI was applied to the diesel engine. A lower air to fuel ratio acts to limit PM oxidation and so it results in higher PM emissions [Tauzia, Maiboom and Shah 10]. From the results obtained by Tauzia et al [2009], shown in figure 12, it is also visible that as the water injection rate increases, so does the PM emissions, this is due to the higher cooling effect at the higher injection rates, which in turn results in less soot oxidising [Tauzia, Maiboom and Shah 10].
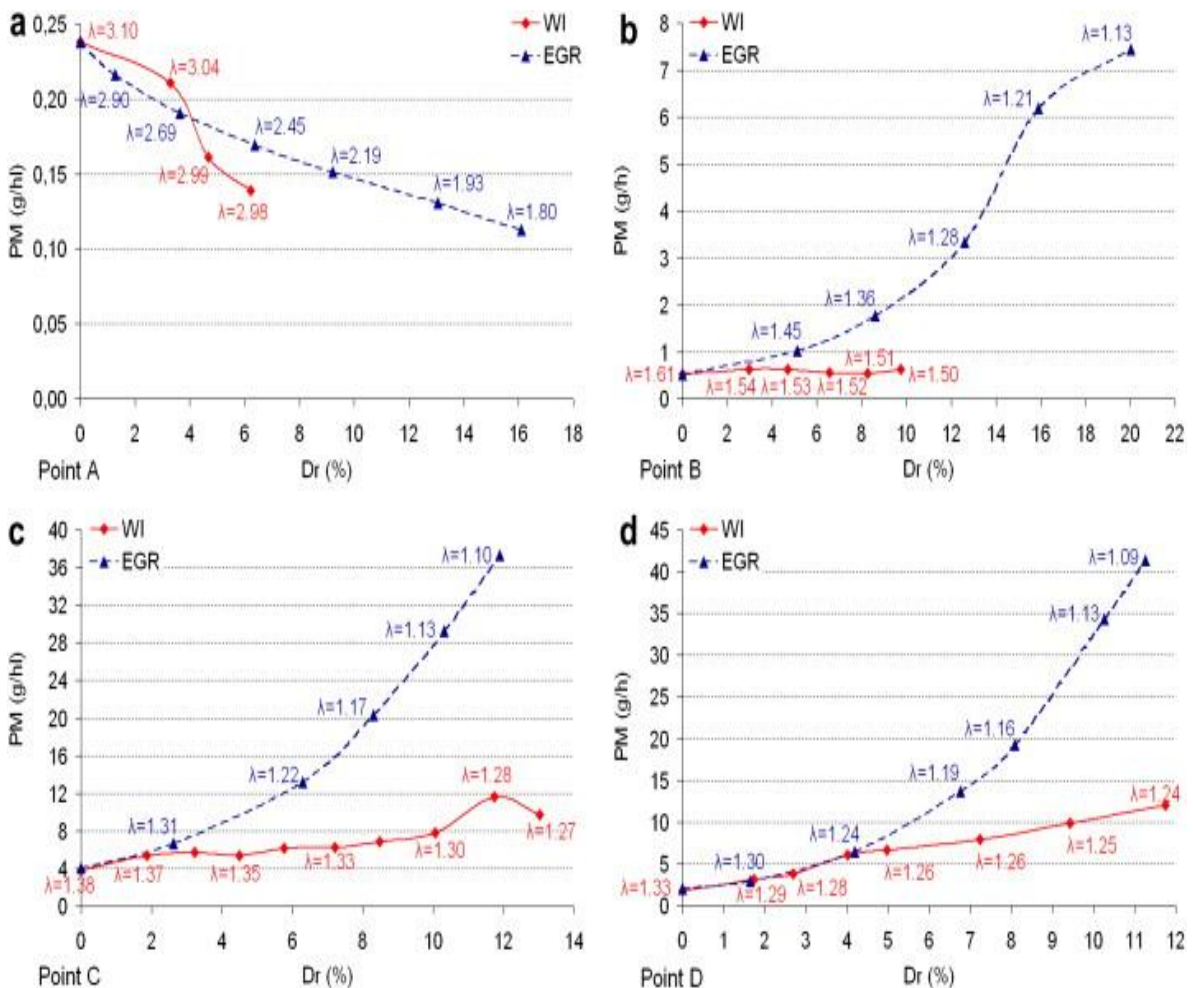
Figure 12. PM emissions vs WI rate (Dr %) for operating loads **a-d** - comparison with EGR [Tauzia, Maiboom and Shah 10].

Contrary to operating loads **b**, **c** and **d**, when the engine was operating under the lower load, load **a**, the PM emissions obtained by Tauzia et al [2009] was seen to decrease when IMWI was applied. The reason for this is that since for the low operation loads the combustion temperature is already low, the addition of WI would result in the temperature becoming even lower. Very low temperatures would then allow the engine to enter a low temperature combustion mode [Tauzia, Maiboom and Shah 10]. Even if the low temperature combustion would mean that soot oxidation would be very limited, the very low combustion temperatures observed at the low combustion mode would become too low for PM formation [Tauzia, Maiboom and Shah 10]. A major drawback though is that at these very low temperatures, CO and HC emissions increase, and the combustion efficiency decreases [Tauzia, Maiboom and Shah 10]. Also seen in figure 12 above, in comparison with EGR, the increase in PM emissions caused by IMWI is much lower.

Overall, from section 3.3, it can be concluded that using IMWI can significantly reduce NOx emissions, however it can also be concluded that using IMWI can increase CO and PM emissions. Therefore, since the Econokit is a novel form of IMWI, with analysing its outputs in this study, it will be determined if it can decrease the NOx emissions without causing an increase in other harmful emissions such as with the other IMWI systems.

3.4 Econokits Catalytic Reactor

The reactor in the Econokit acts as the technology that differentiates it from other IMWI systems. Therefore, to further understand how the Econokit functions and to be able to characterise its outputs in this project, an overview of it is given in this section.

The Econokit reactor is a nickel-iron alloy catalyst [DRAEAUK Ltd 18]. It is mounted on the hottest part of the car engine, usually the exhaust manifold. When water flows from the bubbler as steam into the heated catalytic reactor, the friction caused by the steam on the sides of the reactor causes the potential difference between the hydrogen and oxygen molecules to increase [Econokit France 18]. The polarised water molecules, when injected, act to lower the local temperatures in the engine such as with other IMWI systems, they also act to assist with fuel combustion [Econokit France 18]. With the help of the polarised water molecules fuel can burn completely, which in turn means that less un-burnt gases will exit the engine's exhaust [Econokit France 18].

Mr. Alan Cooper [2018] an innovator in the field of IMWI and an Econokit user has claimed that, when the reactor is subjected to elevated temperatures $200 - 450$ C°, it changes the gas composition [Cooper 18]. He also claims that the Sabatier reaction occurs within these temperatures and that methane is produced [Cooper 18].

3.5 Sabatier Reaction

The Sabatier reaction involves the reaction of carbon dioxide with hydrogen at high temperatures, between 300-400 C° in the presence of a nickel catalyst to produce methane and water [Frontera et al 17].

There are two main reactions involved with the Sabatier reaction [Frontera et al 17], these are:

$$4H_2 + CO_2 \rightarrow CH_4 + 2H_2O \qquad (1)$$
$$3H_2 + CO \rightarrow CH_4 + H_2O \qquad (2)$$

With the side reaction of:

$$H_2 + CO_2 \rightarrow CO + H_2O \qquad (3)$$

Since the Econokit reactor is formed of a nickel catalyst, and since Mr. Alan claims that the Sabatier reaction does occur within the reactor, by performing the gas analysis on the Econokits outputs in this project, it will be determined if these claims are correct and the reaction does indeed occur.

3.6 Methane Injection

Little study has been conducted on injecting methane into the inlet manifold. Methane however has been used in co-combustion as a secondary fuel. If methane is injected by the Econokit into the intake manifold it will combust with the fuel in the combustion chamber in the same as it does in methane-diesel or natural gas-diesel co-combustion.

To analyse the effect of using methane or natural gas for co-combustion with diesel fuel on the engine emissions, Karagoz et al [2016] used different fuel compositions of natural gas

and diesel on a CI engine and analysed the engine emissions. By adding natural gas in the fuel, Karagoz et al [2016] observed an increase in NOx emissions. At lower natural gas compositions, the increase in NOx was slight, however when a fuel mixture consisting of 75% natural gas was used, an increase of 89.4% in NOx emissions was observed by Karagoz et al [2016]. As for CO emissions when Karagoz et al [2016] used a low composition of natural gas in the fuel, an increase in CO emissions was observed, however when a higher natural gas composition was used, 75% natural gas composition, a decrease of 57.1% in CO emissions was observed. For PM emissions, the addition of natural gas in the fuel mixture at all natural gas compositions resulted in a reduction in overall PM emissions, where for a low natural gas composition of 15%, Karagoz et al [2016] observed a 84.8% reduction in PM emissions.

Egúsquiza et al [2009] agrees with Karagoz et al [2016] in that adding natural gas with diesel for co-combustion increases CO emissions. Upon analysing the CO emissions of a DI engine at various natural gas-diesel fuel compositions, the CO emissions were seen to increase significantly at low compositions of natural gas. At higher compositions of natural gas however, of above 75%, same as with Karagoz et al [2016], Egúsquiza et al [2009] observed that the CO emissions decrease. For the NOx emission, on the DI engine, using natural gas for co-combustion, Egúsquiza et al [2009] observed that at all natural gas to diesel fuel compositions the NOx emissions decrease, which is in disagreement with Karagoz et al [2009].

Overall it can be concluded from the results obtained by Karagoz et al [2016] and Egúsquiza et al [2009] that adding methane or natural gas in the combustion chamber would result in an increase in CO emissions and a possible increase in NOx emissions, however adding methane or natural gas would also result in a significant decrease in PM emissions.

4 Test Methodology

The tests performed in this project aim to understand and analyse the yet to be known outputs produced by the Econokit device as the Econokit is subjected to different engine-like conditions. The tests also aim to understand why the Econokit has performed better on some engines as opposed to others in terms of Emission reduction.

To characterise the Econokit device and understand its outputs and what effects its performance, an experimental test bench was set up. The test bench was set up to imitate the same conditions that the Econokit would experience in a car engine. The set-up bench allowed these conditions to be varied to understand their effect of the Econokits outputs and performance.

This section explains in detail; how the test bench was set-up, how the different conditions were varied and how the tests were carried out.

4.1 Experimental Set-Up

The Econokit consists of many different parts, these include, the bubbler, the reactor and the diffuser. Each of these parts are placed in a different part in the engine. They each function in a different way, and the conditions of the engine bay or the engine has a huge influence on how they operate. Therefore, the test bench was created so that each of the Econokits parts are set up in way that they experience the exact same conditions that they would in a vehicle's engine while retaining the ability to vary these conditions. The set-up for each of the Econokits parts is explained in the following sections.

4.1.1 Bubbler Set-Up

The Econokit bubbler, or water tank, is placed in the area under the car bonnet (the engine bay). The water vapour that the air flow picks up as it goes through the bubbler depends on the bubbler's temperature. The temperature of the bubbler depends on the temperature of the engine bay that the Econokit is being used on. A hotter engine bay would mean a hotter bubbler and vice versa.

To imitate the same conditions that the bubbler experiences in an engine, the bubbler in the experimental set up is placed in an ABS 344 x 289 x 117.4mm enclosure, the enclosure acts

as the under-bonnet area heated by the engine (the engine bay), for the bubbler in this set-up. Before placing the bubbler in the enclosure, sixteen 1 cm diameter holes were drilled onto the face of the ABS enclosure, these were drilled to allow air to flow into the enclosure and into the bubbler, they were also drilled to allow for the heating of the enclosure using an external heater fan. Another two 1.5 cm diameter holes were drilled at each side of the enclosure to allow air to recirculate into and out of the enclosure. A final 1.8 cm diameter hole was drilled at the top of the enclosure for the hose connection between the bubbler, inside of the enclosure, and the reactor outside of the enclosure. The enclosure with the 21 drilled holes is shown in figure 13 and 14 below.

Figure 13. ABS enclosure with the 16 holes drilled on the front and the 2 holes drilled on the sides.

Figure 14. ABS Enclosure with the hole drilled at the top for hose connection.

After drilling the holes, the bubbler was filled, and using tape, it was placed in the middle of the ABS enclosure, as shown in figure 15 below.

Figure 15. Econokit bubbler fixed in the ABS enclosure with tape.

To characterise the effect of the engine bay temperature on the bubbler and on the Econokits performance, the temperature inside of the enclosure was varied. To vary the temperature, a Dimplex heater fan was subjected onto the face of the enclosure, as shown in figure 16 below. A thermocouple was placed on the inside of the enclosure, as shown in figure 17 below, and connected to a Fluke 54 B thermocouple reader to give continuous readings of the temperature on the inside of the enclosure.
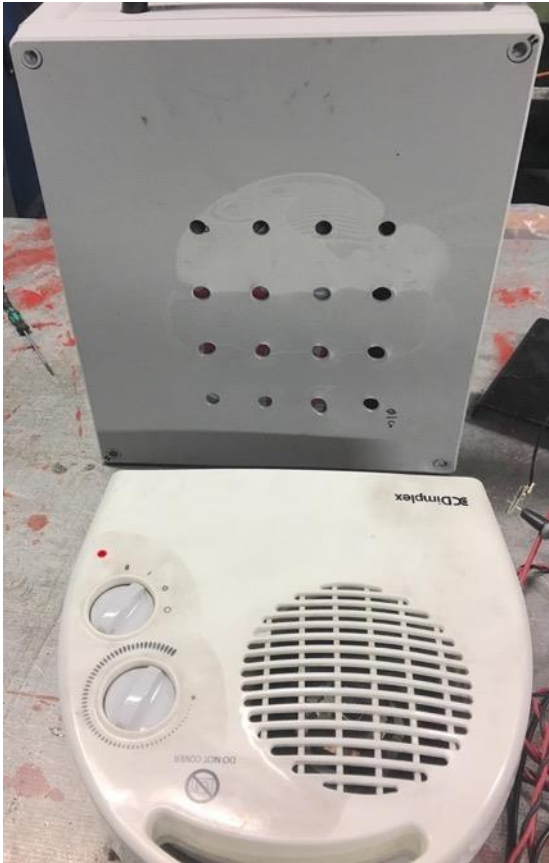
Figure 16. Heater fan subjected onto ABS enclosure to vary enclosure temperature.

Figure 17. Thermocouple placed inside of ABS enclosure for continuous enclosure temperature readings.

This set-up for the bubbler allowed the temperature of the bubbler's ABS enclosure, which acts as the area under the vehicle's bonnet, to be varied using the heater fan, while the temperatures is simultaneously being measured using the thermocouple reader.

4.1.2 Catalytic Reactor Set-Up

The reactor has a huge influence on the Econokits performance. It is where the water is polarised and where the gas composition is expected to change. The reactor is placed on the hottest part of the car engine, the exhaust manifold. The performance of the reactor depends significantly on its temperature. The exhaust manifold temperature however varies from one engine to another which means that the reactor temperature and performance also varies when it is applied on different engines. To characterise the effect of the reactor temperature on the Econokits outputs, the reactor was set up on the test bench in a way that allows its temperature to both be varied and measured simultaneously.

In the set-up, the catalytic reactor is held tightly onto a clamp stand. To apply heat to the reactor and vary its temperature, a Steinel 2000W heat gun was directed at it. To connect the reactor to the rest of the set-up, a hose was used. Hose clamps were used to tighten the hose onto the reactor. Figures 18 below shows the reactor on the clamp with the heat gun directed at it. The heat guns position was also fixed using a clamp.
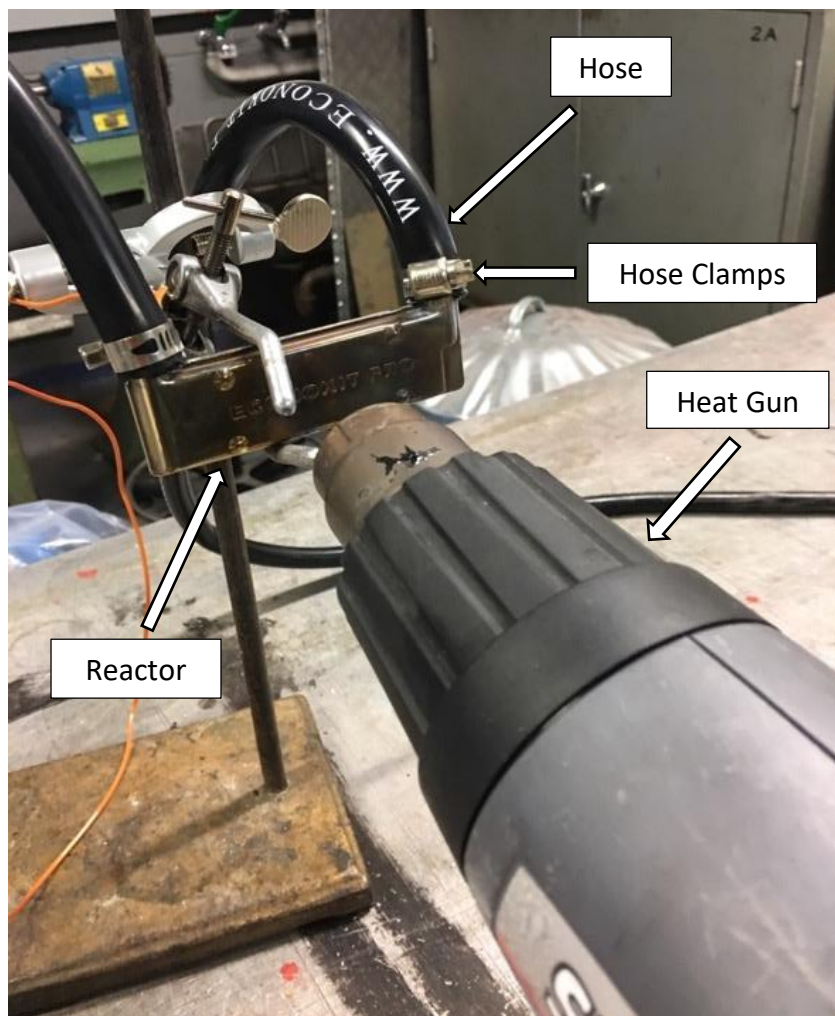
Figure 18. Reactor and heat gun set up.

Temperature readings of the reactor was taken by attaching a thermocouple onto the reactor, this was done by passing the thermocouple through the hose clamps until it was in touch with the reactor, the hose clamps were then tightened holding the thermocouple in place. The thermocouple was then connected to the Fluke 54 B thermocouple reader to allow for continuous readings of the reactor temperature while the temperature was being varied using the heat gun. The attachment of the thermocouple to the reactor is shown in figure 19 below.
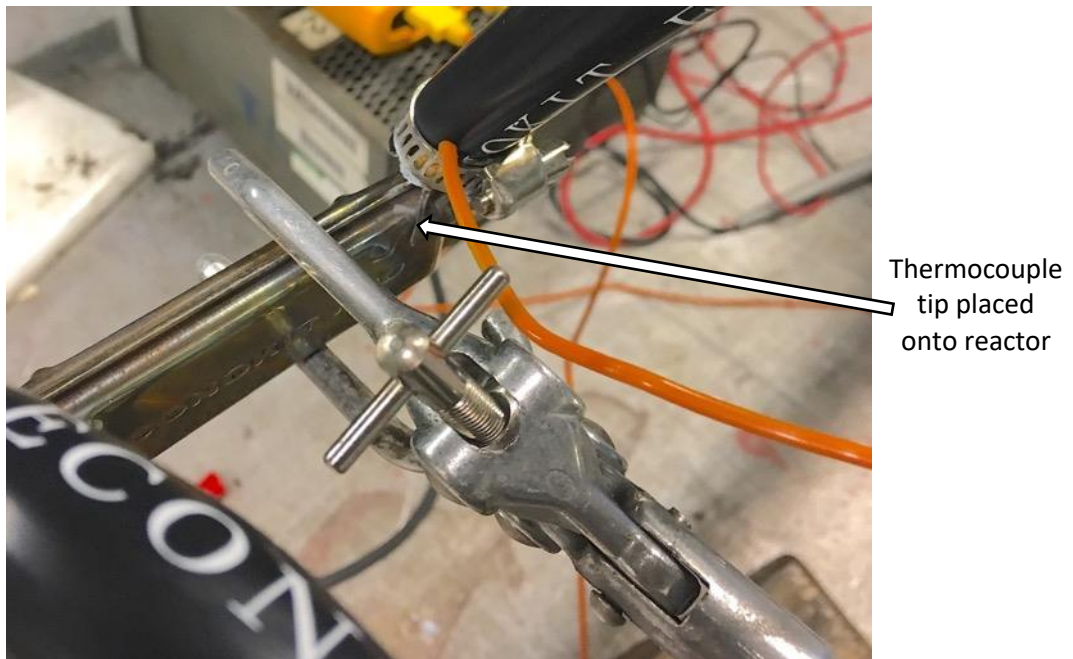
Figure 19. Thermocouple placed onto reactor for reactor temperature readings.

The Steinel heat gun could only however get the reactor's temperature up to 220 C°, where the temperatures for the tests were required to go up to 450 C°. To increase the reactors temperature further and reach the 450 C° mark, a blowtorch was subjected onto the reactor, as shown in figure 20 below.
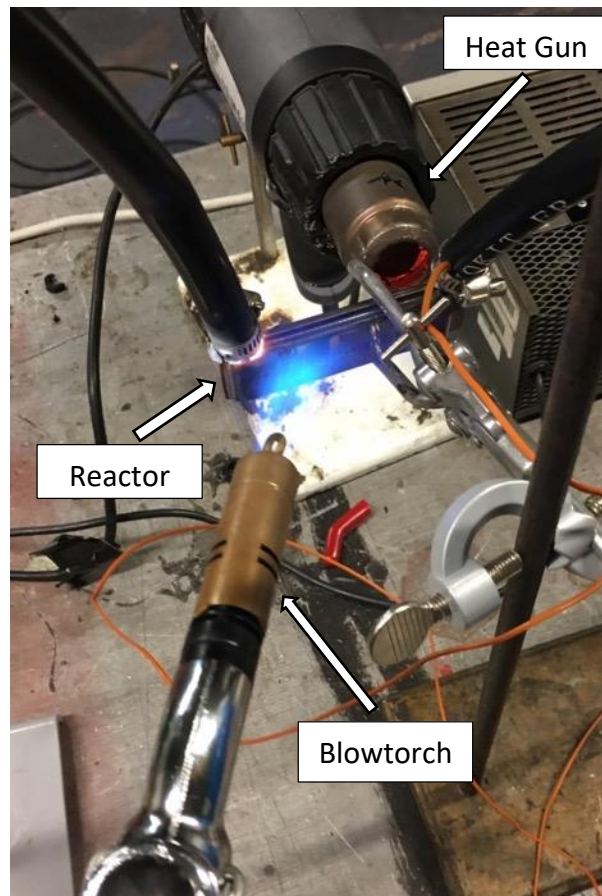
Figure 20. Varying the reactor temperature with heat gun and blowtorch.

4.1.3 Diffuser Set-Up

The diffuser, which is placed into the intake manifold, creates the air flow for the Econokit and injects the Econokits products into the intake manifold. When placed into the intake manifold, using the pressure difference that it creates, the venturi tube diffuser pulls air through the bubbler, through the reactor and into the intake manifold. To simulate the same function of the diffuser, a suction pump was used in the bench set-up. The suction pump was connected at the end of the Econokit setup and was used to act as the diffuser in pulling air through the Econokit device. The air flow rate created by the suction pump was kept constant and was not varied throughout all tests. The suction pump and its connection are shown in figure 21 below.

Figure 21. Suction pump used to stimulate air flow through the Econokit device a) connection between suction pump and Econokit set-up b).

4.1.4 Humidity Sensor Set-Up

To understand and characterise the Econokit device, a humidity sensor was used to measure the water content at the different operating conditions. A TE Connectivity HM1500LF Relative Humidity Sensor was added to the set-up and placed between the bubbler, in its enclosure, and the reactor. To add the humidity sensor to the set-up and get continuous humidity readings without hampering the air flow, the hose connecting the bubbler to the reactor was cut in half and an insertion for the sensor was added in-between. To create the humidity sensor insertion, two pieces of 20 cm long, 22 mm diameter copper pipes were connected together using a brass tee compression fitting, the third connection of the tee fitting was used to insert the humidity sensor. The humidity sensor diameter however is only 12 mm whereas the diameter of the tee fitting in which it would be inserted into is 22 mm.

This means that if the copper pipes with the humidity sensor are added into the Econokit set-up, the air flow will escape out of the tee fitting where the humidity sensor is, which will damage the tests and results. Therefore, a fitting was created for the humidity sensor in the UCL lab, shown in figure 22 below, that allows the sensor to be fitted tightly into the tee fitting without any leakage in the air flow. The copper pipe with the added humidity sensor is shown in figure 23 below.

Figure 22. The humidity sensor and its fittings.

Figure 23. Humidity sensor fitted into copper pipes.

Upon the addition of the sensor to the tee fitting and copper pipes, the pipes were added to the set-up and connected with a hose on each end to the bubbler and reactor. The hose inner diameter however is only 9.5 mm whereas the copper pipe outer diameter is 22 mm. Therefore, to connect the hose to the copper pipe, a hose tail, threaded fitting and a compression fitting were used. The copper pipe with the humidity sensor was then added to the bench set-up between the bubbler and the reactor using the three fittings on each side. The set-up of the three fittings is shown in figure 24 below.
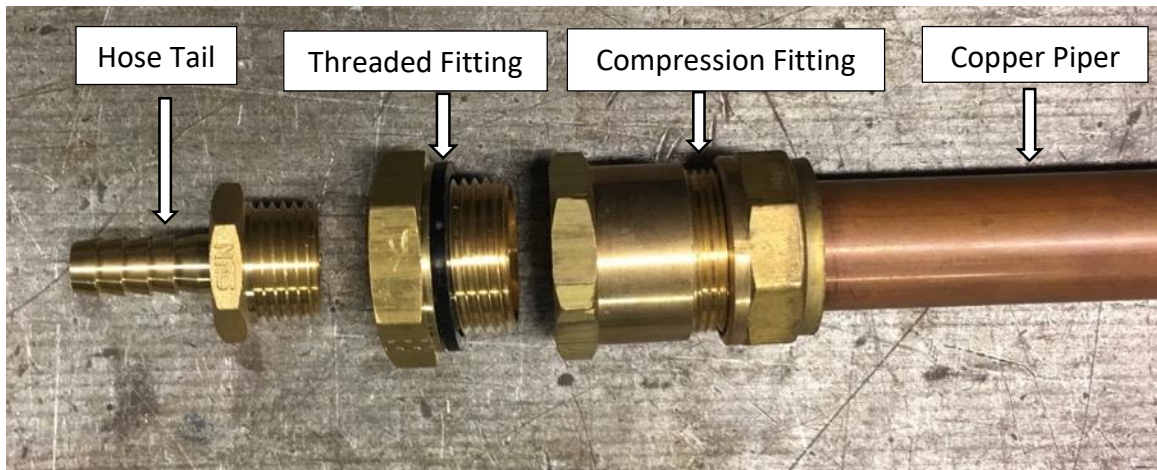
Figure 24. Fittings used to connect Econokit hose to the copper pipe with the humidity sensor.

Upon installing the humidity sensor in the test bench set-up, the sensor was connected to a Metrix MX23 multimeter and a 5V voltage was supplied to it. Continuous readings of the Econokit air flow humidity was then observed as a voltage value from the multimeter. Using the voltage readings, the relative humidity of the air flow was figured by using the voltage to relative humidity reference chart and reference table from the data sheet provided by TE Connectivity which is shown in appendix 3.

4.1.5 Gas Analyser Set-Up

To be able to analyse the gas composition and characterise the effect of bubbler and reactor temperature on the Econokits outputs, a GFM 406 Gas Analyser was added to the bench set-up. The gas analyser was connected at the output of the suction pump using a hose. Using the analyser, readings of CO, CO_2, H_2 and CH_4 were taken at the varying engine conditions.

4.1.6 Full Bench Set-Up

The full set-up of the bench involved the connection of the different parts explained above. The full bench set-up is shown in figure 25 and 26 below.

As seen from figure 25 and 26 below, the set-up consisted of; the bubbler, inside of the enclosure, which is connected to the copper pipe humidity sensor setup, which is connected to the reactor which is then connected to the suction pump that is then connected to the gas analyser. Also seen is the heat gun and fan that are applied to the reactor and enclosure. The blowtorch is not visible in the figure as it was operated manually when the higher reactor temperatures were required.
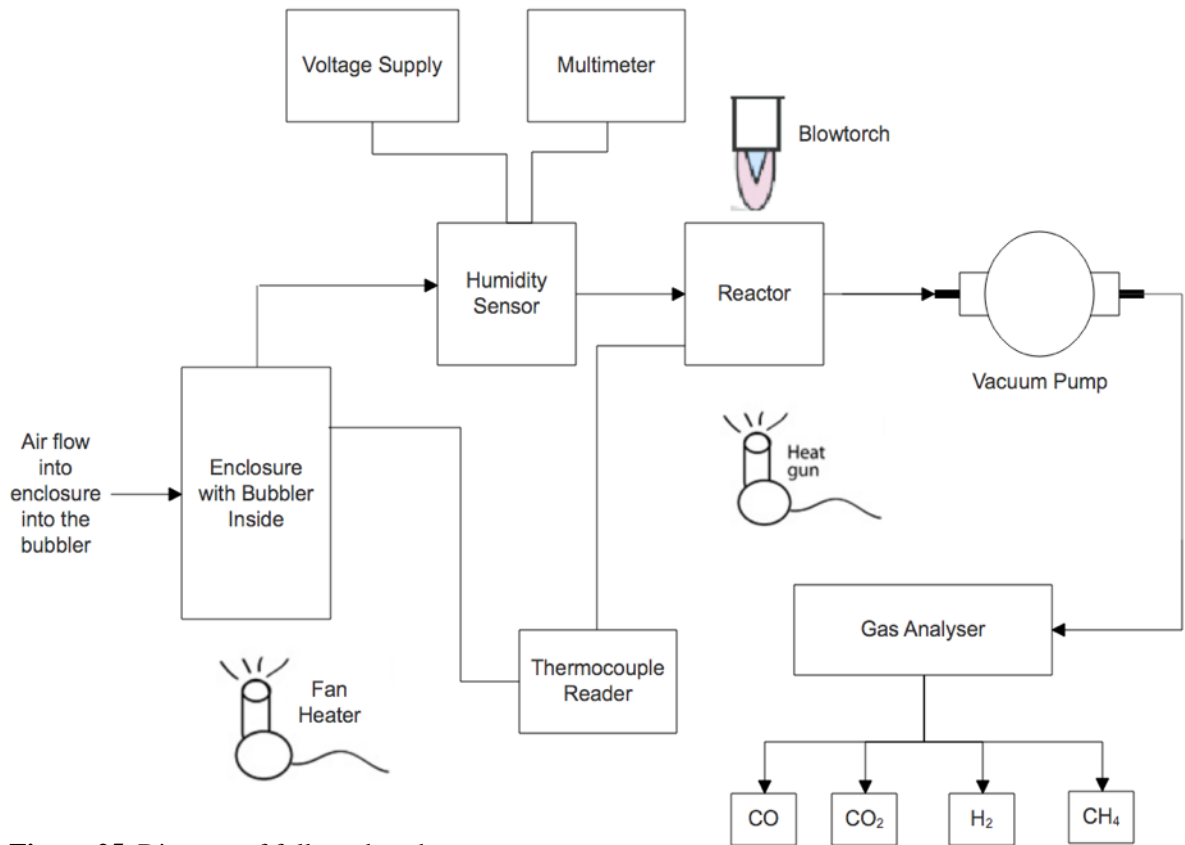
Figure 25. Diagram of full test bench set-up.
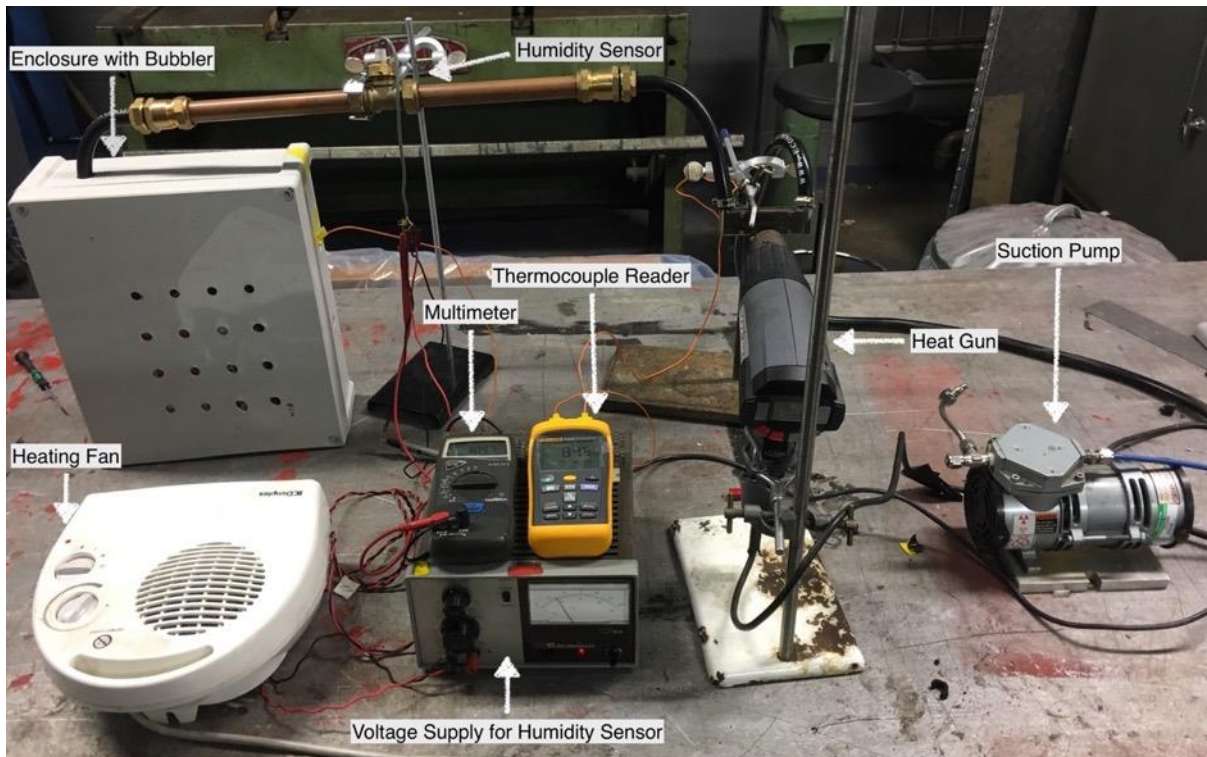
Figure 26. Full in-lab test bench set-up.

4.2 Test Procedure

To understand the outputs of the Econokit and to characterise the effect of bubbler temperature and reactor temperature on the Econokits outputs and performance, two main tests were carried out.

4.2.1 Characterisation of Bubbler Temperature to Water Vapour Content

Using the heater fan in the test bench set-up, shown in figure 26 above, the bubbler temperature was varied. Then using the humidity sensor, the water content in the air flow was noted. The temperature of the enclosure, which acts as the engine bay, was varied from room temperature 23 C° to 65 C°. Using the thermocouple reader, the enclosure temperature was observed, and at intervals of 2 C° the humidity voltage reading was noted. The voltage reading was then transformed to the relative humidity using the reference chart provided. The effect of engine bay temperature on the water content injected by the Econokit was then analysed.

4.2.2 Characterisation of Reactor Temperature to Econokit Outputs

Using the bench set-up, shown in figure 25 and 26 in section 4.1.6 above, the reactor temperature was varied, the gas composition was analysed at the different reactor temperatures. Using both the Steinel heat gun and blowtorch, the temperature of the reactor was varied from $0 - 450$ C°. At temperature intervals of 5 C°, the gas analyser was used to determine the output gas composition. CO, CO_2, CH_4 and H_2 readings were taken with the gas analyser at the varying reactor temperatures. The test was run multiple times and the effect of reactor temperature on the Econokits outputs was analysed.

5 Results and Discussion

In this section, results are given for; the effect of bubbler temperature on the amount and rate of water injected by the Econokit, and the effect of reactor temperature on the gas composition of the Econokits outputs. The results obtained from each of tests are also discussed and analysed in this section.

5.1 Characterisation of Bubbler Temperature to Water Vapour Content

As mentioned earlier, this test was carried out by varying the temperature of the ABS enclosure, which represents the under-bonnet area in a vehicle, from room temperature, 23 °C, to 65 °C. Readings of humidity, or water vapour content, were then taken from the multimeter as voltage values at temperature intervals of 2 °C. The test was run multiple times and the readings for three runs is shown in Table 1 below.

Humidity Readings (mV)			
Enclosure Temperature (C°)	Run 1	Run 2	Run 3
23	2792	2856	2982
25	2832	2869	3012
27	2879	2881	3067
29	2884	2892	3078
31	2880	2898	3086
33	2887	2901	3105
35	2890	2939	3128
37	2906	2952	3187
39	2939	2969	3226
41	2987	2961	3265
43	2995	2997	3357
45	3023	3054	3382
47	3065	3114	3378
49	3087	3151	3369
51	3103	3201	3365
53	3134	3231	3359
55	3122	3236	3356
57	3175	3246	3359
59	3205	3305	3376
61	3267	3342	3390
63	3289	3358	3416
65	3303	3364	3433

Table 1. Humidity in mV of Econokit air flow vs enclosure temperature.

Table 1 above shows the readings of the relative humidity of the air flow in the Econokit set-up as the temperature of the enclosure was varied for three different runs. The readings were taken in mV off of the multimeter. To get the relative humidity % from the voltage values, the reference graphs and table provided by TEConnectivity, shown in appendix 3, were used.

To accurately find the relative humidity, along with the table and graphs mentioned above, the following equation, which was also provided in the data sheet for the sensor, was used:

$$Relative\ Humidity\ (\%) = 0.03892\ V_{out}(mV) - 42.017 \qquad (4)$$

Using the equation given, the relative humidity of the Econokit air flow at the different enclosure temperatures was calculated and is given in table 2 below.

Relative Humidity (%)			
Enclosure Temperature (C°)	Run 1	Run 2	Run 3
23	66.65	69.14	74.04
25	68.20	69.64	75.21
27	70.03	70.11	77.35
29	70.23	70.54	77.78
31	70.07	70.77	78.09
33	70.35	70.89	78.83
35	70.46	72.37	79.72
37	71.08	72.87	82.02
39	72.37	73.54	83.54
41	74.24	73.23	85.06
43	74.55	74.63	88.64
45	75.64	76.84	89.61
47	77.27	79.18	89.45
49	78.13	80.62	89.10
51	78.75	82.57	88.95
53	79.96	83.73	88.72
55	79.49	83.93	88.60
57	81.55	84.32	88.72
59	82.72	86.61	89.38
61	85.13	88.05	89.92
63	85.99	88.68	90.93
65	86.54	88.91	91.60

Table 2. Relative humidity of Econokit air flow vs enclosure temperature.

As seen in table 2 above, as the temperature of the enclosure increased, so did the relative humidity of the air flow. Also seen from the table is that the relative humidity values were different from one run to the other, for example at the enclosure temperature of 23 C°, the relative humidity for runs 1, 2 and 3 were 66.65%, 69.14% and 74.04% respectively. The difference in relative humidity between runs is mainly attributed to the fact that the runs were completed on three different days. The relative humidity of the atmosphere before starting the runs on each of the three days was different, thus for each of the runs the starting relative humidity before the Econokit effecting the humidity of the air flow was different. Therefore, given in table 3 below is the relative humidity of the atmosphere on the three different days of which the test was run. By using table 3 below, the effect of the bubbler temperature on the relative humidity of the Econokit air flow, shown in table 2, can be better understood.

	Run 1	Run 2	Run 3
Relative Humidity (%)	55.36084	60.61504	65.013

Table 3. Relative humidity of atmosphere on the day of which each run was conducted.

The aim of this test however is to characterise the effect of the engine bay temperature on the bubbler and in turn on the water content injected by the Econokit. Although the results for the relative humidity of the air flow, shown in table 2 above, give an indication to the effect of enclosure temperature on water content, it does not give the actual water content and injection rate for the Econokit. Therefore, to find the direct effect of enclosure temperature on the water injected, the absolute humidity of the air flow is calculated. The absolute humidity represents the total mass of vapour present in a m^3 of air. So, when calculated, the absolute humidity gives the mass of water vapour present in a m^3 of air flowing through the Econokit and into the intake manifold. Since the air flow injection rate of the Econokit is constant, the absolute humidity also gives the Econokit water injection rate, a higher absolute humidity for the Econokit air flow for example would mean that more water is being injected by the Econokit into the manifold per unit time.

The absolute humidity of the air flow for the different enclosure temperatures was calculated with the following equations [Vaisala 13]:

$$Absolute\ Humidity = C * \frac{P_W}{T_1} \tag{5}$$

Where,

$$P_W = P_{WS}(T_2) * Relative\ Humidity\ \%$$ (6)

And,

$$P_{WS} = A * 10^{\frac{m*T_2}{T_2+T_n}}$$ (7)

P_W = Vapour pressure in Pa
P_{WS} = Water vapour saturation pressure in hPa
C = Constant 2.16679 gK/J
T_1 = Temperature in K
T_2 = Temperature in C°
A, m, T_n = constants, given in appendix 4

Using the equations shown above and the relative humidity % values given in table 2, the absolute humidity was calculated at the different enclosure temperatures for the three different runs and is shown in table 4 and figure 27 below.

Absolute Humidity (g/m³)			
Enclosure Temperature (C°)	Run 1	Run 2	Run 3
23	13.70	14.21	15.22
25	15.70	16.03	17.31
27	18.02	18.04	19.91
29	20.17	20.26	22.34
31	22.43	22.65	25.00
33	25.05	25.24	28.07
35	27.87	28.62	31.53
37	31.18	31.97	35.98
39	35.15	35.72	40.57
41	39.86	39.32	45.67
43	44.19	44.24	52.55
45	49.43	50.22	58.56
47	55.60	56.97	64.36
49	61.80	63.77	70.48
51	68.31	71.62	77.16
53	76.02	79.61	84.35
55	82.73	87.35	92.21
57	92.79	95.93	100.93
59	102.75	107.59	111.02
61	115.31	119.27	121.80
63	126.85	130.81	134.14
65	138.85	142.66	146.97

Table 4. Absolute humidity of air flow vs enclosure temperature.
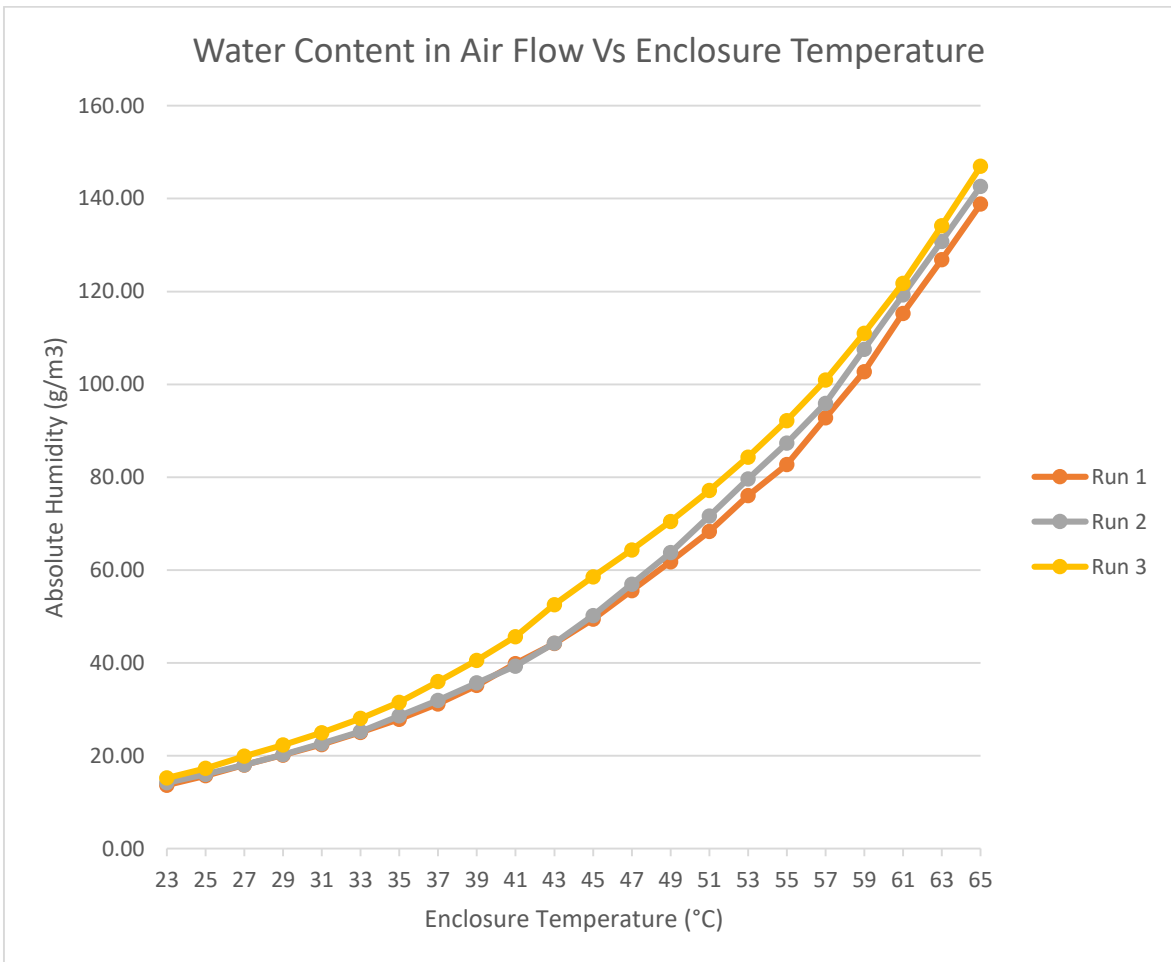
Figure 27. Absolute humidity vs Enclosure temperature.

As seen in table 4 and figure 27 above, the temperature of the enclosure, which represents the temperature of the under-bonnet area in a vehicle, has a huge effect on the amount and rate of water being injected by the Econokit. Remarkably, what was seen is that for all three runs, the mass of water per m^3 of air being injected increased significantly from enclosure temperature 23 °C to enclosure temperature 65 °C. Where for the three runs, the mass of water per m^3 of air flow was 13.70 g, 14.21 g and 15.22 g at enclosure temperature 23 °C, whereas when the enclosure temperature was increased to 65 °C, the mass of water per m^3 of air flow was seen to increase to 138.85 g, 142.66 g and 146.97 g for each of the runs respectively. It is also seen from figure 27 that the increase in amount of water in a m^3 of the air flow increased in an exponential matter with the increase in enclosure temperature. Since the Econokit injection air flow rate does not change, as mentioned earlier, the absolute humidity also represents the water injection rate, and so as seen from table 4 and figure 27, as the enclosure temperature increases the water injection rate increases, again in an exponential matter.

The main reason for the increase in water vapour content in the air flow as the enclosure temperature, or engine bay temperature, is increased is attributed to the fact that when the enclosure or engine bay temperature is higher, the temperature of the water inside of the bubbler is also higher. A higher temperature for the water inside the bubbler would mean that the water evaporates and turns into water vapour at a quicker rate. A higher evaporation rate at the higher bubbler temperatures would therefore mean that for a constant injection air flow rate, such as that of the Econokit, more water vapour is being added per m^3 of air passing through the bubbler.

The increase in absolute humidity of the air flow observed, which is about a 10 time increase between the two enclosure temperatures of 23 °C and 65 °C, is massive, and gives an explanation as to why the Econokit is very effective on reducing emissions when applied in some engines but is not as effective in other engines. From the results, it is seen that if the Econokit and the Econokit bubbler are placed on a vehicle with a low engine bay temperature, it will not inject much water into the manifold, the water injection rate will also be low. If the Econokit and the bubbler are however placed on a vehicle with a high engine bay temperature, more water will be injected by the Econokit in a period of time, the water injection rate will be higher.

From the literature reviewed and from section 3.3 specifically, it is seen that the water injection rate for an IMWI system, such as the Econokit, has a huge effect on the emissions. As explained in section 3.3, a higher water injection rate will result in higher NOx emission reductions, it also however results in slightly higher PM and CO emissions. Therefore, since, as seen from the results, the water injection rate of the Econokit depends substantially on the bubbler temperature; to control the injected rate of the Econokit and control the vehicle's emissions, the temperature of the bubbler must be carefully monitored, controlled and adjusted. As mentioned, the results give an indication as to why the Econokit has not been very significant with emission reductions on some engines, if the engine bay temperature of the vehicle that the Econokit is being used on is too low, the bubbler temperature will also be low, and the injection rate could be too slow for the Econokit to have an effect on the engine emissions. Therefore, to ensure that the water injection rate of the Econokit is sufficient, for a vehicle with a low engine bay temperature, the bubbler should be installed onto a hotter component in the engine so that its temperature would high enough for an adequate water injection rate.

5.2 Characterisation of Reactor Temperature to Econokit Outputs

The outputs of the Econokit that are injected into the intake manifold include water and a processed gas. The processed gas, produced in the catalytic reactor, is unknown. In this test, the gas output of the Econokit is analysed at different reactor temperatures. The temperature of the reactor was varied from $0 - 450$ °C and at intervals of 5 °C, CO, CO_2, H_2 and CH_4 emissions in the Econokit output were measured using the gas analyser.

5.2.1 Carbon Dioxide Detection

The test was run to measure the amount of CO_2 in the output of the Econokit at the varying reactor temperatures. The test was performed multiple times and CO_2 was indeed detected in the output gas at high reactor temperatures. CO_2 concentration readings were obtained at the varying reactor temperature as a % volume of the output gas composition using the gas analyser. The % volume concentration was then converted to volumetric parts per million (ppm). The results for the CO_2 concentration in the output air flow at the different reactor temperatures for three runs is given in figure 28 below. Also given on figure 28 is the mean CO_2 concentration at the varying reactor temperatures.
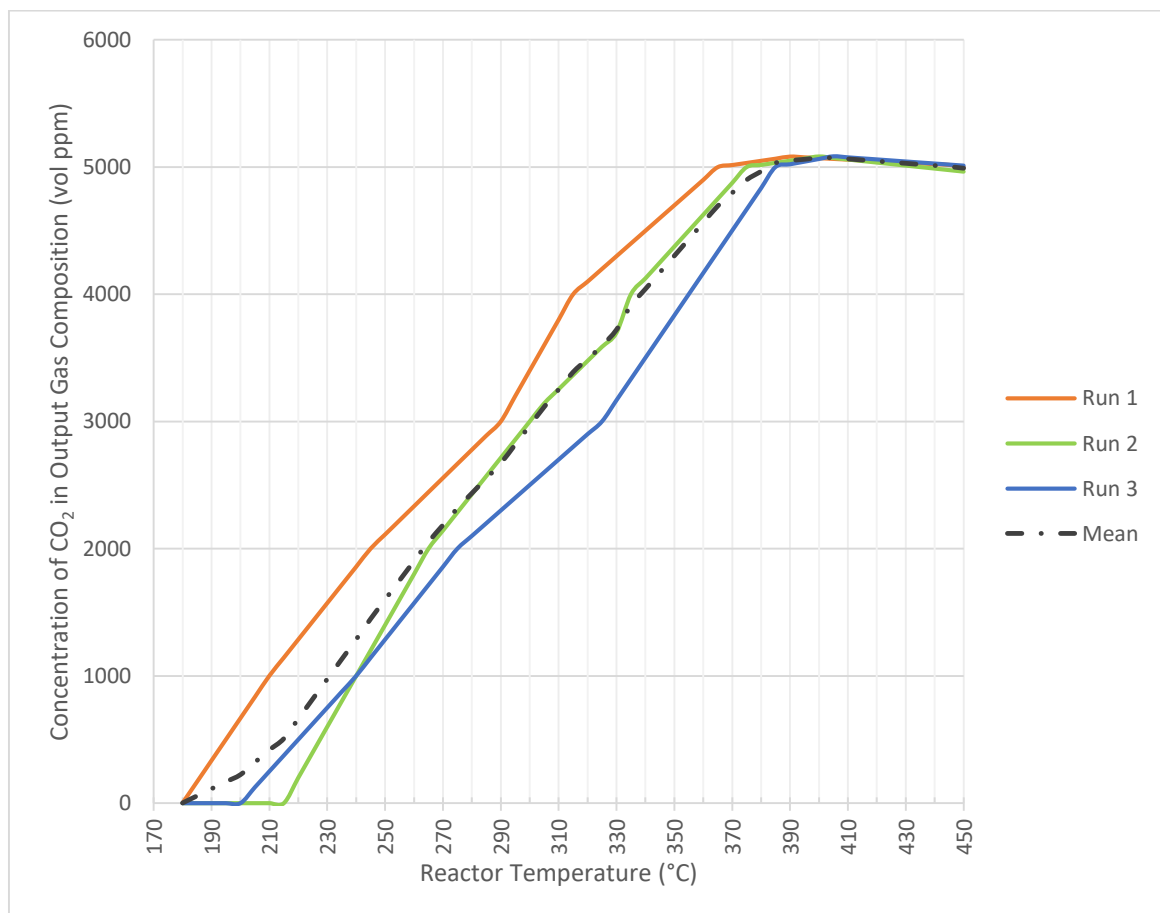
Figure 28. Concentration of CO_2 in Econokit output air flow vs Reactor temperature.

As seen in figure 28 above, the reactor did indeed change the composition of the output air flow of the Econokit. For reactor temperatures up to 180 °C, the reactor did not produce any CO_2 gas. However, when the reactor temperature reached 180 °C, as seen for Run 1 in figure 28 above, the reactor started to change the gas composition and produce CO_2. As for Run 2 and 3, it can be seen from figure 28 that the reactor also produced CO_2, however the CO_2 production began from reactor temperatures of 215 °C and 200 °C respectively. The results above therefore show that when the reactor temperature reaches 180 – 215 °C, it will start to affect the output gas composition and produce CO_2 gases which are then injected into the intake manifold.

Also seen from figure 28 is that the concentration of CO_2 in the output flow increased with the increase in reactor temperature. The maximum amount of CO_2 concentration observed in the air flow was around 5100 ppm for all three runs. For Run 1,2 and 3, the maximum CO_2 concentration in the output air flow was observed at reactor temperatures between 380 °C and 410 °C, as seen in figure 28. When the temperature of the reactor was further increased however, a very slight decrease in CO_2 concentration was observed.

There are two logical explanation as to why CO_2 is produced in the reactor, these are; either the carbonates in the water vapour in the air flow decompose at higher reactor temperatures to form CO_2, or the rubber hose attached to the reactor oxidises at the high reactor temperatures to form CO_2. To understand whether the CO_2 is produced from the oxidising of the rubber hose or from the decomposition of the carbonates in the water vapour, the reactor temperature was again varied and the CO_2 composition in the output air flow was analysed however with the reactor disconnected from the water tank. When the reactor was disconnected from the water tank, no CO_2 was detected in the output flow at all reactor temperatures and therefore this indicates that the CO_2 produced is from the decomposition of the carbonates in the water vapour flowing through the heated reactor and not from the oxidising of the rubber hose.

To understand the variability of data and to determine the variation of CO_2 production expected from the reactor at each reactor temperature, the standard deviation from the mean and the coefficient of variance for the CO_2 output at each reactor temperature was calculated. In appendix 5, the standard deviation and the coefficient of variance of CO_2 at each reactor temperature is given, shown in table 5 below however is a summary of the calculations. In

the summary in table 5 below, for a given range of reactor temperatures, the range of values of SD and CV calculated for each of the temperatures in that range is given.

Range of Reactor Temperatures	SD of the CO_2 Output from the Mean (ppm)	CV of the CO_2 Output from the Mean (%)	Average of SD in Temperature Range (ppm)	Average of CV in Temperature Range (%)
From 180 °C to 225 °C	From 96.225 to 582.573	From 173.205 to 66.115	401.783	136.041
From 230 °C to 380 °C	From 116.644 to 600.338	From 53.702 to 2.348	428.106	17.58
From 385 °C to 450 °C	From 9.038 to 33.298	From 0.661 to 0.178	17.920	0.355

Table 5. Summary of standard deviation and co-efficient of variance for CO_2 concentration in output air flow at each reactor temperature.

From table 5 above, it can be seen that for low reactor temperatures, the standard deviation and the coefficient of variance for the CO_2 output from the mean CO_2 output, shown in figure 28, is high. This means that the CO_2 output at the low reactor temperatures can vary from the mean given in figure 28, however the variation would have little significance as at the low reactor temperatures the CO_2 output is already low and insignificant in affecting engine emissions and with any deviation in the concentration of CO_2 at these low reactor temperatures, the CO_2 output would still remain insignificant in affecting engine emissions. Also seen from table 5 above, is that for higher reactor temperatures, where the CO_2 production is high, both the SD and the CV are low, therefore this indicates that at the high reactor temperatures there will be little variation in the concentration of CO_2 produced from the mean in figure 28 above, and that the concentration of CO_2 in the Econokits injected output will always be precisely close to 5100 ppm at these high reactor temperatures.

Overall, from the results it is seen that, if the reactor temperature is above 180 °C, it will produce CO_2 with a concentration of up to 5100 ppm, which means that with the water vapour being injected by the Econokit into the manifold, CO_2 will also be injected with a concentration of up to 5100 ppm. As seen from the literature review, section 3.1.1, one of the methods used to lower engine emissions is EGR. EGR injects CO_2 and CO into the intake manifold to reduce NO_x emissions. The concentration of 5100 ppm detected in the Econokit output air flow at the high reactor temperatures indicates that the Econokit might be able to

induce the effect of EGR in emissions reduction through the injected CO_2. However, whether the 5100 ppm of CO_2 injected by the Econokit would be sufficient to induce the effects of EGR or not depends on the engine that the Econokit is being used on and the mass of the total intake air mixture of that engine. If the 5100 ppm of CO_2 introduced accounts to a significant percentage of the total intake air mass of the engine then it would be effective in inducing the effects of EGR explained in section 3.1.1, if the 5100 ppm of CO_2 is insignificant in regard to the mass of the total intake air mixture of the engine however, then it will not induce the effects of EGR.

5.2.2 Carbon Monoxide Detection

The test was again run multiple times to detect the concentration of CO in the output air flow at the different reactor temperatures. Figure 29 below shows the CO concentration in the output air flow at the different reactor temperatures for three different runs. Also given on figure 51 is the mean CO concentration at the varying reactor temperatures.
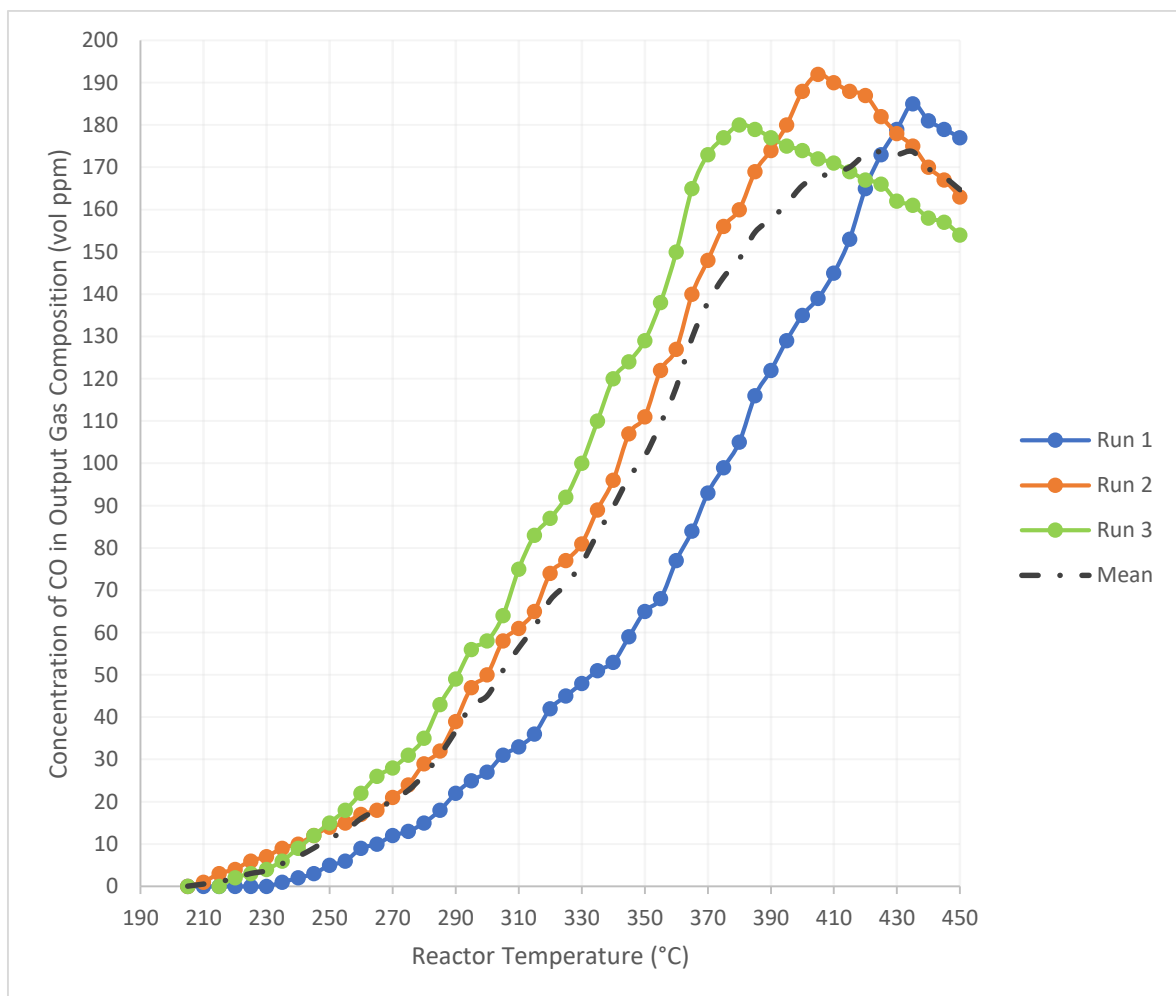
Figure 29. Concentration of CO in Econokit output air flow vs Reactor temperature.

As seen from figure 29 above, at elevated temperatures, the reactor produces CO gas. From temperatures of 220 °C, 215 °C and 205 °C for Run 1,2 and 3 respectively, CO was detected in the output gas composition. As the temperature of the reactor was increased, the CO concentration was also seen to increase. For Run 1 the maximum concentration of CO obtained, 185 ppm, was achieved at reactor temperature 425 °C. For Run 2 and 3 however the maximum concentration of CO obtained was 192 and 180 ppm and were obtained at reactor temperature 405 °C and 380 °C respectively. For the three runs it was seen that upon reaching the maximum concentration of CO at the reactor temperatures mentioned, any further increase in reactor temperature would act to reduce the CO concentration in the output air flow composition. As explained in section 5.2.1 above, the reason for the CO production in the Econokits reactor, is the same as that for the CO_2 production, which is at the high reactor temperatures, carbonates in the water vapour passing through the reactor decompose to form CO.

Again, to understand the variability of data and to determine the variation of CO production expected from the reactor at each reactor temperature, the standard deviation from the mean and the coefficient of variance for the CO output at each reactor temperature was calculated. Shown in table 6 below is the summary for the calculated SD and CV of CO concentration in Econokit air flow output at the reactor temperatures. The SD and CV at each reactor temperature is shown in appendix 6.

Range of Reactor Temperatures	SD of the CO Output from the Mean (ppm)	CV of the CO Output from the Mean (%)	Average of SD in Temperature Range (ppm)	Average of CV in Temperature Range (%)
From 205 °C to 235 °C	From 0.5774 to 4.0414	From 75.78 to 173.21	2.4771	119.66
From 240 °C to 350 °C	From 4.3588 to 33.9460	From 32.46 to 62.27	16.8768	40.25
From 355 °C to 450 °C	From 8.0208 to 41.4769	From 4.62 to 24.94	24.9365	17.03

Table 6. Summary of standard deviation and co-efficient of variance for CO concentration in output air flow at each reactor temperature.

As seen from table 6 above, for low reactor temperatures, the CV is high. The SD is however very low at the lower reactor temperatures and indicates that the even if the CO concentration at the low temperatures can vary considerably from the mean of CO output sown in figure 29 above, the amount of which the CO will vary will not have a significant influence on the effect of the injected CO. For higher reactor temperatures, where the CO production and concentration is also higher, it is seen from table 6 that the SD for CO outputs is also higher. The CV however is lower at the higher reactor temperatures and indicates that at these temperatures the CO produced and injected would be similar to that shown on the mean curve in figure 29 above.

Overall from the results of CO concentration, is seen that if the reactor temperature is between 390 – 430 °C, it can produce CO at a concentration of up to 192 ppm. However, this amount indicates that the CO produced by the reactor, which is then injected into the intake manifold, is insufficient for it to have an effect on emissions in the same way that it does in the EGR system. In the EGR system, CO is injected in the intake manifold to reduce engine emissions. The amount of CO produced by the Econokit however would be insignificant in instigating the effects of EGR. Although the CO injected by the Econokit does not have a huge effect on engine emissions, it will combust in the combustion chamber which will in turn increase engine power.

5.2.3 Hydrogen Detection

The test was run multiple times to detect the concentration of H_2 in the output air flow at the varying reactor temperatures. Figure 30 below shows the concentration of H_2 in the output air flow at the different reactor temperatures for three different runs conducted. Also shown on figure 30 is the mean H_2 concentration at the varying reactor temperatures.
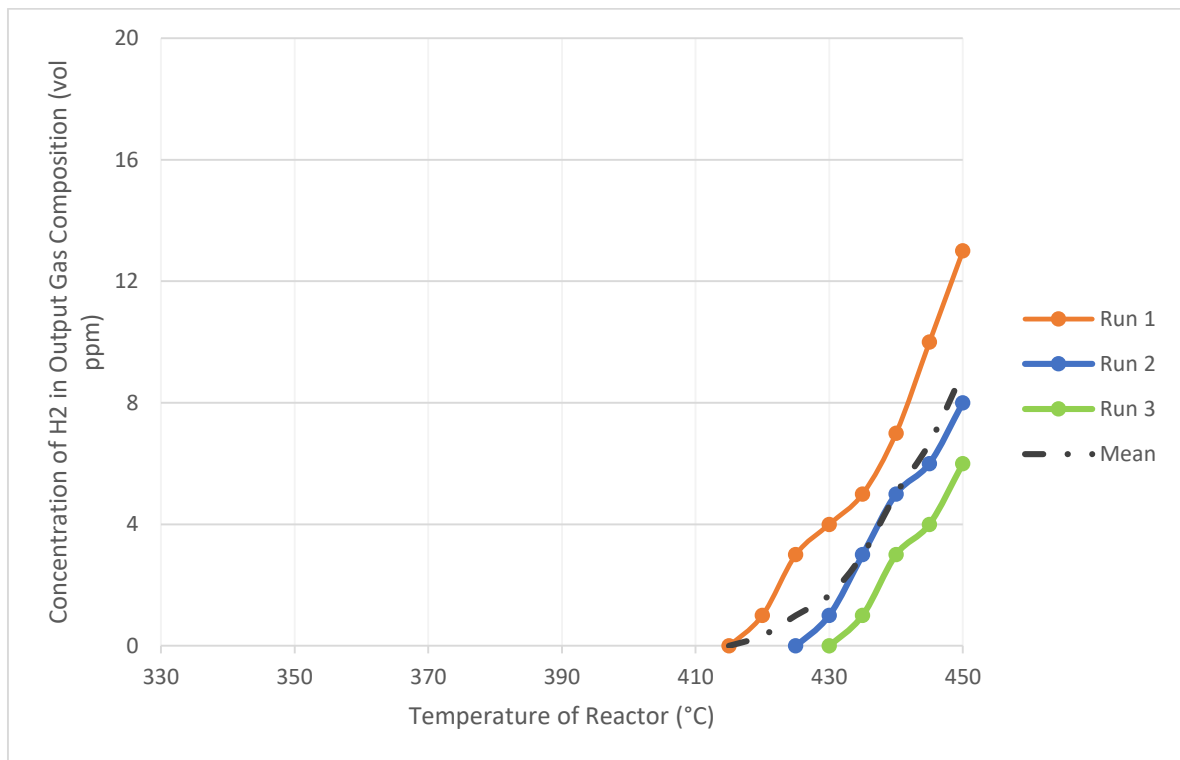
Figure 30. Concentration of H_2 in Econokit output air flow vs Reactor temperature.

As seen in figure 30 above, at very high temperatures, the reactor also produces H_2. For Run 1, hydrogen was detected from reactor temperature 415 °C, whereas for Run 2 and 3, hydrogen was detected at reactor temperatures 420 °C and 430 °C. Also seen from figure 30 is that when the reactor temperature reached maximum temperature, 450 °C, the concentration of H_2 in the output was 13 ppm, 8 ppm and 6 ppm for Runs 1, 2 and 3 respectively. This shows that even though H_2 is produced in the reactor, the amount produced is minimal and would not have an effect on the engine emissions when injected into the manifold. From the results however, it is also seen that as the temperature is increased, the concentration of H_2 also increases. This indicates that if the reactor temperature is further increased, above 450 °C, there would be a higher concentration of H_2 where it can reach a point where it can be high enough to affect the engine emissions.

If the reactor temperature does increase above 450 °C and the H_2 production becomes sufficient, this will mean that Econokit is injecting H2, CO, CO_2. These three gases are the constituents of syngas, therefore at very high reactor temperatures, the Econokit would be injecting syngas. Syngas when injected would act as a secondary fuel in the combustion chamber [Feng 17]. It assists in combustion, and when injected it would act to reduce PM emissions by achieving more complete combustion and would also act to increase the engine power [Feng 17].

5.2.4 Methane Detection

The tests were again run multiple times, this time to detect the concentration of methane in the output gas composition at the varying reactor temperatures. Upon varying the temperature of the reactor from $0 - 450$ °C for the multiple runs, no methane was detected.

CO however was detected in the output gas composition, as shown in section 5.2.2 above, CO is a by-product of the Sabatier reaction, as shown in section 3.5. Also, the gas analyser used to detect methane has a minimum detection level of 10000 ppm, and so the detection of CO indicates that the Sabatier reaction might have occurred, however the methane produced might have had a concentration of less than 10000 ppm and so was not detected by the gas analyser. If the methane however was produced at a concentration of less than 10000 ppm, it would still not be enough to affect the engine emissions upon injection into the intake manifold. For future work however, to confirm whether the methane was produced at a concentration lower than 10000 ppm, a gas analyser with a lower minimum methane detection should be used.

5.2.5 Effect of Reactor Temperature on Injected Water Content

Overall, from the gas analysis tests conducted in section 5.2, it can be seen that at high reactor temperatures, the reactor produces CO_2, CO and H_2 which are injected into the intake manifold. However, it should also be noted that for all the gas analysis tests carried out, section 5.2, as the reactor temperature was increased, the water content in the air flow was seen to slightly decrease. This means that although at elevated reactor temperatures the Econokit produces and injects CO_2, CO and H_2 into the intake manifold, when the reactor is at these elevated temperatures, the amount of water being injected decreases. As discussed in literature section 3.3.1, the higher the water injection rate, the more the IMWI system will reduce NOx emissions. Therefore, the slight reduction in water injection rate observed when the reactor temperature was increased could mean that at the higher reactor temperatures the effect of the Econokit in NOx emissions reduction could be reduced.

6 Conclusion

With the aim of characterising and understanding the Econokit device, a test bench was set up. The test-bench was set up to simulate the same conditions that the Econokit experiences on an engine, with the ability to alter and change these conditions. Two main tests were carried out, these are; the characterisation of the effect of bubbler temperature on water injection rate and the characterisation of the effect of reactor temperature on Econokit outputs.

From the first test it was clear that the temperature of the bubbler has a huge effect on the amount of water injected and the water injection rate of the Econokit. It was seen that as the bubbler temperature was increased, so did the water injection rate. When the temperature of the bubbler enclosure, which represents the under-bonnet area in a vehicle, was increased from 23 °C to 65 °C, the water injection rate experienced up to a significant 10 times increase.

In the second test, the reactor temperature was varied from 0 – 450 °C and the output gas composition was analysed. From the tests it was clear that the reactor does indeed change the composition of the Econokit output gas. When the reactor temperature was between 180 °C and 220 °C, both CO_2 and CO were produced and detected in the output composition. As the temperature of the reactor was further increased, the concentration of CO_2 and CO in the output flow was also seen to increase, where at reactor temperatures between 380 °C and 420 °C, the concentration of CO_2 and CO in the Econokit output flow was up to 5100 ppm and 192 ppm respectively. From the gas analysis tests, it was also seen the reactor produces H_2, at elevated reactor temperatures, above 415 °C, H_2 was detected in the gas analyser. The concentration of hydrogen detected however was minimal, where it only reached up to 13 ppm at the reactor temperature of 450 °C. The tests were also run to detect methane in the output composition, however no methane was detected at all reactor temperatures. CO detection however indicates that there might have been methane in the output gas, however with a concentration too little to be detected by the gas analyser. Also, although it was observed that the Econokit produces CO_2, CO and H_2, it was also seen however that at the high reactor temperatures, when these gases are produced, the amount of water injected by the Econokit reduces, a lower water injection rate could mean that the Econokits performance in reducing NOx emissions would be reduced.

Overall from the results of both tests, the elements that differentiate the Econokit from other IMWI systems can be seen. The high CO_2 concentration, of 5100 ppm, at the high reactor temperatures indicates that the Econokit can reduce the engine emissions by acting as an IMWI system through the injection of water, but that it also has the potential to reduce the engine emissions by inducing the effects of an EGR system through the injected CO_2. However, whether the CO_2 produced and injected could affect the engine in the same way as in EGR depends on the engine that the Econokit is used on and the intake air mass of that engine as discussed in section 5.2.1. Also, as seen, both CO and H_2 are produced and injected by the Econokit. These two gases are the constituents of syngas. Syngas when injected into the intake manifold also acts to reduce NOx emissions. Additionally, CO and syngas, when injected into the intake manifold, they will act as a secondary fuel and will combust in the combustion chamber, this allows for more complete combustion and thus less PM emissions and will also generate additional engine power.

Through both the literature reviewed and the tests conducted, multiple explanations as to why the Econokits performance in reducing engine emissions has varied when applied on different vehicles, can be given. From the literature reviewed it can be concluded that the performance of an IMWI system, such as the Econokit, in reducing emissions depends on multiple factors, these include; the engine type and engine load. The Econokit will be more effective on reducing engine emissions for an engine running on a high load than an engine running on a low load, if the engine load is too low, the effect of an IMWI system on reducing emissions, NOx emissions in particular, can become negligible. From the tests, an explanation can also be given to the variance in Econokit performance. As seen from the results, the water injection rate of the Econokit depends significantly on the temperature of the bubbler, and since the performance of an IMWI depends substantially on the water injection rate, as seen from the literature, this indicates that the performance of the Econokit will depend on the temperature of the engine bay it is placed in. A high engine bay temperature would result in a higher bubbler temperature and so a higher water injection rate, whereas a low engine bay temperature would result in a lower bubbler temperature and a lower water injection rate. Also seen is that for the Econokit reactor to change the gas composition and produce CO_2, CO and H_2, it needs to be at a very high temperature. Therefore, whether the Econokit will inject these gases into the intake manifold or not will depend on the exhaust manifold temperature of the engine that the Econokit is applied to.

7 Future Work

Suggestions for future work include:

- Ramp the reactor temperatures to even higher than 450 °C to check if at the higher temperatures more H_2 is produced.
- Further analyse the amounts of H_2 and CO produced to determine if they will be sufficient to induce the effects of syngas upon injection into the intake manifold.
- Analyse the emissions of an engine upon applying the Econokit while ensuring; that the bubbler temperature is higher than 60 °C, to ensure maximum water injection rate, and while ensuring that the reactor temperature is above 400 °C, to ensure that the output gases mentioned above are being produced and injected.
- Compare the effect of the Econokit on an engine's emissions; with the reactor applied, and with the reactor disconnected. As seen in this study, the reactor acts to introduce CO_2, CO and H_2 into the intake manifold, however at the same time the reactor also reduces the amount of water being injected by the Econokit. Therefore, it should be analysed whether using the reactor and introducing these gases with a lower water injection rate would cause a larger reduction in engine emissions or disconnecting the reactor and ensuring a higher water injection rate would cause a larger reduction in engine emissions.

References

Arruga, H., Scholl, F., Kettner, M., Amad, O., Klaissle, M. and Giménez, B. (2017). Effect of intake manifold water injection on a natural gas spark ignition engine: an experimental study. *IOP Conference Series: Materials Science and Engineering*, 257, p.012029.

Babu, A., Amba Prasad Rao, G. and Hari Prasad, T. (2015). Direct injection of water mist in an intake manifold spark ignition engine. *International Journal of Automotive and Mechanical Engineering*, 12, pp.2809-2819.

Bureau Veritas (2018). *Efficiency Test of Econokit System*. [online] Econokit.fr. Available at: http://www.econokit.fr/wp-content/uploads/2016/06/Bureau-Veritas_synth-by-Econokit_ENG_.pdf [Accessed 30 Aug. 2018].

Collie, S. (2018). *BMW water injection system offers improved performance and fuel economy*. [online] Newatlas.com. Available at: https://newatlas.com/bmw-water-injection-efficiency-power/38289/ [Accessed 31 Aug. 2018].

Cooper, A. (2018). *Econokit Reactor*. [email].

Department for Transport (2018). *Vehicle licensing statistics: 2017*. United Kingdom: Department for Transport.

DRAEAUK Ltd (2018). *Materials Analysis*. DRAEAUK Ltd.

Econokit France (2018). *Econokit - système efficace contre la pollution de nos véhicules*. [online] ECONOKIT. Available at: http://www.econokit.fr/?lang=en [Accessed 30 Aug. 2018].

Econokit India (2013). *ECONOKIT - FUEL SAVER - POLLUTION SAVER - REDUCE POLLUTION AND SAVE FUEL - REMOVE BLACK SMOKES - EXTEND ENGINE LIFESPAN - THE ECONOKIT TECHNOLOGY*. [online] Econokit-india.com. Available at: http://econokit-india.com/home/login/11-about-us [Accessed 30 Aug. 2018].

EPA (2018) a. *Sources of Greenhouse Gas Emissions*. United States: Environmental Protection Agency.

EPA (2018) b. *Global Greenhouse Gas Emissions Data*. United States: Environmental Protection Agency.

Egúsquiza, J., Braga, S. and Braga, C. (2009). Performance and gaseous emissions characteristics of a natural gas/diesel dual fuel turbocharged and aftercooled engine. *Journal of the Brazilian Society of Mechanical Sciences and Engineering*, 31(2), pp.142-150.

FARAG, M., KOSAKA, H., BADY, M. and ABDEL-RAHMAN, A. (2017). Effects of intake and exhaust manifold water injection on combustion and emission characteristics of a DI diesel engine. *Journal of Thermal Science and Technology*, 12(1), pp.JTST0014-JTST0014.

Feng, S. (2017). Numerical Study of the Performance and Emission of a Diesel-Syngas Dual Fuel Engine. Mathematical Problems in Engineering, 2017, pp.1-12.

Fernando, S., Hall, C. and Jha, S. (2006). NOxReduction from Biodiesel Fuels. *Energy & Fuels*, 20(1), pp.376-382.

Frontera, P., Macario, A., Ferraro, M. and Antonucci, P. (2017). Supported Catalysts for CO2 Methanation: A Review. *Catalysts*, 7(12), p.59.

Gabbattis, J. (2018). *Transport is UK's most polluting sector as greenhouse gas emissions fall*. [online] The Independent. Available at: https://www.independent.co.uk/environment/air-pollution-uk-transport-most-polluting-sector-greenhouse-gas-emissions-drop-carbon-dioxide-a8196866.html [Accessed 30 Aug. 2018].

Government of Canada (2017). *Greenhouse gas emissions: drivers and impacts*. Canada: Government of Canada.

Government of Canada (2018). Air pollution: regulations for vehicles and engines. Canada: Government of Canada.

Greeves, G., Khan, I. and Onion, G. (1977). Effects of water introduction on diesel engine combustion and emissions. *Symposium (International) on Combustion*, 16(1), pp.321-336.

Hull, R. (2018). *There will be almost 200k electric cars on UK roads by the end of 2018*. [online] This is Money. Available at: http://www.thisismoney.co.uk/money/cars/article-5246793/There-200-000-electric-cars-UK-roads-2018.html [Accessed 30 Aug. 2018].

Ibrahim, A. and Bari, S. (2009). A comparison between EGR and lean-burn strategies employed in a natural gas SI engine using a two-zone combustion model. *Energy Conversion and Management*, 50(12), pp.3129-3139.

International Energy Agency (2012). *CO2 Emissions from Fuel Combustion 2012*. Paris: Organisation for Economic Co-operation and Development

Junaedi, C. (2011). Compact and Lightweight Sabatier Reactor for Carbon Dioxide Reduction. *NASA*.

Karagöz, Y., Sandalcı, T., Koylu, U., Dalkılıç, A. and Wongwises, S. (2016). *Effect of the use of natural gas–diesel fuel mixture on performance, emissions, and combustion characteristics of a compression ignition engine*. Advances in Mechanical Engineering, 8(4), p.168781401664322.

Kettner, M., Dechent, S., Hofmann, M., Huber, E., Arruga, H., Mamat, R. and Najafi, G. (2016). *Investigating the influence of water injection on the emissions of a diesel engine*.

Khalilarya, S., Jafarmadar, S., Khatamnezhad, H. and Javadirad, G. (2011). Simultaneously Reduction of NOx and Soot Emissions in a DI Heavy Duty diesel Engine Operating at High Cooled EGR Rates. *International Journal of Mechanical and Mechatronics Engineering*, 5(9)

Khirsariya, P. and Mewada, R. (2013). Single Step Oxidation of Methane to Methanol–Towards Better Understanding. *Procedia Engineering*, 51, pp.409-415.

Leahy, S. (2018). *Electric Cars May Rule the World's Roads by 2040*. [online] News.nationalgeographic.com. Available at: https://news.nationalgeographic.com/2017/09/electric-cars-replace-gasoline-engines-2040/ [Accessed 30 Aug. 2018].

Lindley, T. (2016). *An Investigation into the Effects of the EconoKit on the Engine Performance and Fuel Efficiency of an Agricultural Tractor*. Postgraduate. University of Bristol.

Ma, X., Zhang, F., Han, K., Zhu, Z. and Liu, Y. (2014). Effects of Intake Manifold Water Injection on Combustion and Emissions of Diesel Engine. *Energy Procedia*, 61, pp.777-781.

Mingrui, W., Thanh Sa, N., Turkson, R., Jinping, L. and Guanlun, G. (2017). Water injection for higher engine performance and lower emissions. *Journal of the Energy Institute*, 90(2), pp.285-299.

Mira LTD and PBA (2002). EMISSION CONTROL TECHNOLOGY FOR HEAVY-DUTY VEHICLES. [online] Available at: http://Some of the disadvantages associated with a high-pressure system include the fouling of components exposed to the un-processed exhaust gases, pressure differentials associated with turbocharged engines and backpressure from particulate traps. It is anticipated that a high-pressure system with particulate trap could meet Euro 4 emissions standards with 15% EGR rate at full load [Accessed 31 Aug. 2018].

Public Health England (2014). *Estimates of mortality in local authority areas associated with air pollution*. [online] Available at: https://www.gov.uk/government/news/estimates-of-mortality-in-local-authority-areas-associated-with-air-pollution [Accessed 1 Sep. 2018].

Sarvi, A., Kilpinen, P. and Zevenhoven, R. (2009). Emissions from large-scale medium-speed diesel engines: 3. Influence of direct water injection and common rail. *Fuel Processing Technology*, 90(2), pp.222-231.

Sher, E. (1998). *Handbook of Air Pollution from Internal Combustion Engines*. San Diego: Academic Press.

Statista (2018). *Worldwide number of electric cars 2017 | Statista*. [online] Statista. Available at: https://www.statista.com/statistics/270603/worldwide-number-of-hybrid-and-electric-vehicles-since-2009/ [Accessed 30 Aug. 2018].

SUBRAMANIAN, V., MALLIKARJUNA, J. and RAMESH, A. (2007). Effect of water injection and spark timing on the nitric oxide emission and combustion parameters of a hydrogen fuelled spark ignition engine. *International Journal of Hydrogen Energy*, 32(9), pp.1159-1173.

Tauzia, X., Maiboom, A. and Shah, S. (2010). Experimental study of inlet manifold water injection on combustion and emissions of an automotive direct injection Diesel engine. *Energy*, 35(9), pp.3628-3639.

Tesfa, B., Mishra, R., Gu, F. and Ball, A. (2012). Water injection effects on the performance and emission characteristics of a CI engine operating with biodiesel. *Renewable Energy*, 37(1), pp.333-344.

Tolleson, J. (2018). *US environment agency declares greenhouse gases a threat*. [online] Nature International Weekly Journal of Science. Available at: https://www.nature.com/news/2009/090417/full/news.2009.374.html [Accessed 30 Aug. 2018].

Tschalamoff, T., Laaß, U. and Janicke, D. (2007). Direct water injection in a medium speed gas engine. *MTZ worldwide*, 68(11), pp.15-18.

Union of Concerned Scientists. (2018). *Cars, Trucks, Buses and Air Pollution*. [online] Available at: https://www.ucsusa.org/clean-vehicles/vehicles-air-pollution-and-human-health/cars-trucks-air-pollution#.W4hF-GaZOMK [Accessed 30 Aug. 2018].

Vehicle Certificate Agency (2018). *Cars and air pollution*. Bristol: Vehicle Certificate Agency.

Wartsila (2018). *Direct Water Injection (DWI)*. [online] Wartsila.com. Available at: https://www.wartsila.com/encyclopedia/term/direct-water-injection-(dwi) [Accessed 31 Aug. 2018].

Westfall, C. (2018). *How It Works: Water Methanol Injection.*[Online] Diesel Army. Available at: https://www.dieselarmy.com/engine-tech/how-it-works/how-it-works-water-methanol-injection/ [Accessed 1 Sep. 2018].

What's Your Impact. (2018). *Effects of increased greenhouse gas emissions*. [online] Available at: https://whatsyourimpact.org/effects-increased-greenhouse-gas-emissions#footnote2_g72mad0 [Accessed 30 Aug. 2018].

Wildhaber, S. (2011). *Impact of combustion phasing on energy and availability distributions of an internal combustion engine*. Masters. Missouri University of Science and Technology.

Neslen, A. (2018). *Electric cars emit 50% less greenhouse gas than diesel, study finds*. [online] The Guardian. Available at: https://www.theguardian.com/environment/2017/oct/25/electric-cars-emit-50-less-greenhouse-gas-than-diesel-study-finds [Accessed 30 Aug. 2018].

Zhang, Z., Kang, Z., Jiang, L., Chao, Y., Deng, J., Hu, Z., Li, L. and Wu, Z. (2017). Effect of direct water injection during compression stroke on thermal efficiency optimization of common rail diesel engine. *Energy Procedia*, 142, pp.1251-1258.

Zheng, M., Reader, G. and Hawley, J. (2004). Diesel engine exhaust gas recirculation—a review on advanced and novel concepts. *Energy Conversion and Management*, 45(6), pp.883-900.

Appendix

1) Fuel characteristics for section 3.2.1

Table 3. Test—fuel properties

		LFO	HFO
Density (15 °C)	kg/m^3	834	940
Viscosity (80 °C)	mm^2/s	3.32	66.6
HHV	MJ/kg	45.5	43.2
LHV	MJ/kg	42.8	41.1
CCAI	–	806	857
Enthalpy of vapor	kJ/kg	~ 287	~ 252
Stoich. air/fuel ratio	kg/kg	14.3	13.8
H/C ratio	mol/mol	1.96	2.06
Aromaticity	vol %	~ 14	~ 78
Cetane number	–	~ 50	~ 35
FBP	°C	~ 355	~ 577

[Sarvi et al 09

2) Engine loads a-d for section 3.3.1 and 3.3.3

Table 2
Operating points.

Point	A	B	C	D
Engine speed (rpm)	1500	1665	2050	2000
Torque (N m)	45	114	140	200
Pilot quantity (mg/stroke)	1.2	1.5	1.7	2.4
Principal quantity (mg/stroke)	11.2	22.8	30.7	39.7
BMEP (bar)	2.8	7.1	9.5	12.7
P_{rail} (bar)	600	865	1028	1154

[Tauzia et al 10]

3) Reference chart and table to calculate relative humidity for section 4.4.1 and 5.1

• **Modeled Signal Output**
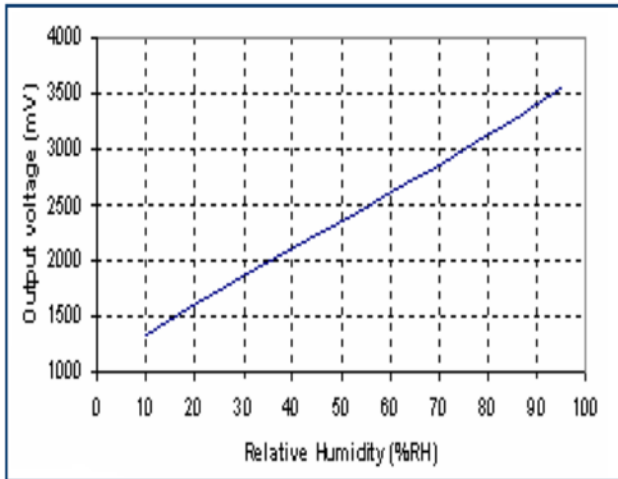
RH (%)	Vout (mV)	RH (%)	Vout (mV)
10	1325	55	2480
15	1465	60	2605
20	1600	65	2730
25	1735	70	2860
30	1860	75	2990
35	1990	80	3125
40	2110	85	3260
45	2235	90	3405
50	2360	95	3555

4) Constants used to calculate absolute humidity is section 5.1

	A	m	Tn	max error	Temperature range
water	6.116441	7.591386	240.7263	0.083%	-20...+50°C
	6.004918	7.337936	229.3975	0.017%	+50...+100°C
	5.856548	7.27731	225.1033	0.003%	+100...+150°C
	6.002859	7.290361	227.1704	0.007%	+150...+200°C
	9.980622	7.388931	263.1239	0.395%	+200...+350°C
	6.089613	7.33502	230.3921	0.368%	0...+200°C
ice	6.114742	9.778707	273.1466	0.052%	-70...0°C

[Vaisala 13]

5) Standard deviation and co-efficient of variance for CO_2 concentration at each reactor temperature (section 5.2.1)

	A	B	C	D	E	J	K
1							
2	Reactor Temperature	Run 1 CO2 (g/m3)	Run 2 CO2 (g/m3)	Run 3 CO2 (g/m3)	Mean	Standard Deviation	CV
39	180	0	0	0	0	0	
40	185	166.6666667	0	0	55.55555556	96.22504486	173.20508
41	190	333.3333333	0	0	111.1111111	192.4500897	173.20508
42	195	500	0	0	166.6666667	288.6751346	173.20508
43	200	666.6666667	0	0	222.2222222	384.9001795	173.20508
44	205	833.3333333	0	125	319.4444444	449.4080469	140.68426
45	210	1000	0	250	416.6666667	520.4164999	124.89996
46	215	1142.857143	0	375	505.952381	582.5736063	115.14396
47	220	1285.714286	200	500	661.9047619	560.6725796	84.705929
48	225	1428.571429	400	625	817.8571429	540.726552	66.115037
49	230	1571.428571	600	750	973.8095238	522.9592666	53.702419
50	235	1714.285714	800	875	1129.761905	507.5995596	44.929782
51	240	1857.142857	1000	1000	1285.714286	494.8716593	38.490018
52	245	2000	1200	1142.857143	1447.619048	479.2284048	33.104594
53	250	2111.111111	1400	1285.714286	1598.941799	447.2173514	27.969583
54	255	2222.222222	1600	1428.571429	1750.26455	417.618213	23.860291
55	260	2333.333333	1800	1571.428571	1901.587302	390.9791573	20.560674
56	265	2444.444444	2000	1714.285714	2052.910053	367.9436751	17.92303
57	270	2555.555556	2142.857143	1857.142857	2185.185185	351.1250799	16.068436
58	275	2666.666667	2285.714286	2000	2317.460317	334.4651985	14.432402
59	280	2777.777778	2428.571429	2100	2435.449735	338.9412373	13.916988
60	285	2888.888889	2571.428571	2200	2553.439153	344.7965917	13.503223
61	290	3000	2714.285714	2300	2671.428571	351.9624284	13.175064
62	295	3200	2857.142857	2400	2819.047619	401.3582382	14.23737
63	300	3400	3000	2500	2966.666667	450.9249753	15.199718
64	305	3600	3142.857143	2600	3114.285714	500.6118705	16.074693
65	310	3800	3253.968254	2700	3251.322751	550.0047718	16.916339
66	315	4000	3365.079365	2800	3388.359788	600.3386408	17.717677
67	320	4100	3476.190476	2900	3492.063492	600.1574497	17.186327
68	325	4200	3587.301587	3000	3595.767196	600.0447899	16.687532
69	330	4300	3698.412698	3166.666667	3721.693122	567.0252152	15.235679
70	335	4400	4000	3333.333333	3911.111111	538.8602512	13.777677
71	340	4500	4125	3500	4041.666667	505.1814855	12.499336
72	345	4600	4250	3666.666667	4172.222222	471.5027198	11.300997
73	350	4700	4375	3833.333333	4302.777778	437.8239541	10.175379
74	355	4800	4500	4000	4433.333333	404.1451884	9.1160569
75	360	4900	4625	4166.666667	4563.888889	370.4664227	8.117341
76	365	5000	4750	4333.333333	4694.444444	336.787657	7.1741749
77	370	5016.649155	4875	4500	4797.216385	266.9631162	5.5649588
78	375	5033.29831	5000	4666.666667	4899.988325	202.747236	4.1377086
79	380	5049.947465	5016.649155	4833.333333	4966.643318	116.6441524	2.348551
80	385	5066.59662	5033.29831	5000	5033.29831	33.29830977	0.6615604
81	390	5083.245774	5049.947465	5020.811444	5051.334894	31.24028068	0.6184559
82	395	5077.299648	5066.59662	5041.622887	5061.839718	18.30789154	0.3616845
83	400	5071.353521	5083.245774	5062.434331	5072.344542	10.44105543	0.2058428
84	405	5065.407394	5071.362925	5083.245774	5073.338698	9.081834137	0.179011
85	410	5059.461267	5059.480075	5075.125854	5064.689066	9.038528812	0.1784617
86	415	5053.515141	5047.597226	5067.005934	5056.039433	9.947538656	0.1967457
87	420	5047.569014	5035.714376	5058.886013	5047.389801	11.58685798	0.2295614
88	425	5041.622887	5023.831527	5050.766093	5038.740169	13.69672446	0.2718284
89	430	5035.67676	5011.948678	5042.646173	5030.090537	16.09311886	0.319937
90	435	5029.730634	5000.065828	5034.526253	5021.440905	18.66600971	0.3717262
91	440	5023.784507	4988.182979	5026.406332	5012.791273	21.35168829	0.4259441
92	445	5017.83838	4976.300129	5018.286412	5004.14164	24.11249671	0.4818508
93	450	5000	4964.41728	5010.166492	4991.527924	24.02248231	0.4812651

5) Standard deviation and co-efficient of variance for CO concentration at each reactor temperature (section 5.2.2)

	A	B	C	D	E	J	K
1							
2	Reactor Temperature	Run 1 CO (g/m3)	Run 2 CO (g/m3)	Run 3 CO (g/m3)	Mean	Standard Deviation	CV
45	210	0	1	0	0.333333	0.577350269	173.2050808
46	215	0	3	0	1	1.732050808	173.2050808
47	220	0	4	2	2	2	100
48	225	0	6	3	3	3	100
49	230	0	7	4	3.666667	3.511884584	95.77867048
50	235	1	9	6	5.333333	4.041451884	75.77722283
51	240	2	10	9	7	4.358898944	62.26998491
52	245	3	12	12	9	5.196152423	57.73502692
53	250	5	14	15	11.33333	5.507570547	48.59621071
54	255	6	15	18	13	6.244997998	48.03844614
55	260	9	17	22	16	6.557438524	40.98399078
56	265	10	18	26	18	8	44.44444444
57	270	12	21	28	20.33333	8.020806277	39.44658825
58	275	13	24	31	22.66667	9.073771726	40.03134585
59	280	15	29	35	26.33333	10.26320288	38.97418815
60	285	18	32	43	31	12.52996409	40.41923899
61	290	22	39	49	36.66667	13.65039682	37.22835496
62	295	25	47	56	42.66667	15.94783162	37.37773036
63	300	27	50	58	45	16.09347694	35.76328209
64	305	31	58	64	51	17.57839583	34.46744281
65	310	33	61	75	56.33333	21.38535324	37.96216552
66	315	36	65	83	61.33333	23.71356855	38.66342698
67	320	42	74	87	67.66667	23.15887159	34.22493338
68	325	45	77	92	71.33333	24.00694344	33.65459361
69	330	48	81	100	76.33333	26.31222783	34.47016746
70	335	51	89	110	83.33333	29.90540642	35.88648771
71	340	53	96	120	89.66667	33.94603561	37.85803227
72	345	59	107	124	96.66667	33.70954365	34.87194171
73	350	65	111	129	101.6667	33.00505012	32.46398372
74	355	68	122	138	109.3333	36.67878588	33.54767001
75	360	77	127	150	118	37.32291521	31.62958916
76	365	84	140	165	129.6667	41.4769012	31.98732741
77	370	93	148	173	138	40.92676386	29.65707526
78	375	99	156	177	144	40.36087214	28.02838343
79	380	105	160	180	148.3333	38.83726733	26.18242741
80	385	116	169	179	154.6667	33.8575447	21.8906539
81	390	122	174	177	157.6667	30.92463958	19.61393631
82	395	129	180	175	161.3333	28.11286775	17.42533125
83	400	135	188	174	165.6667	27.46512941	16.57854894
84	405	139	192	172	167.6667	26.76440422	15.96286534
85	410	145	190	171	168.6667	22.5905585	13.39361176
86	415	153	188	169	170	17.52141547	10.30671498
87	420	165	187	167	173	12.16552506	7.032095411
88	425	173	182	166	173.6667	8.020806277	4.618506493
89	430	179	178	162	173	9.539392014	5.51409943
90	435	185	175	161	173.6667	12.05542755	6.941704921
91	440	181	170	158	169.6667	11.50362262	6.780131209
92	445	179	167	157	167.6667	11.01514109	6.569666657
93	450	177	163	154	164.6667	11.59022577	7.038598644